WPI

Design of a low-profile home speaker using a moving magnet transducer and passive radiators

Jack Arabian
(jharabian@wpi.edu)

Heath Bastow
(hbastow@wpi.edu)

Rion Crear
(rscrear@wpi.edu)

Keira Lynch
(kxlynch@wpi.edu)

A Major Qualifying Project submitted to the faculty of
Worcester Polytechnic Institute
in partial fulfillment of the requirement for the
Degree in Bachelor of Science in Mechanical Engineering

Submitted to:
Professor Joe Stabile, Worcester Polytechnic Institute

Abstract

For this Major Qualifying Project, the team's main goal was to design and create a working low-profile bass speaker. The team first reviewed previous years' work in creating this speaker and discovered the airtightness of their speakers was not maintained and their actuator motors were not sufficiently robust. Based on these issues with the previous years' speakers, the team conducted modifications to improve the speaker housing and actuator designs. These modifications were done first using SolidWorks for the first iterations of designs, then Fusion360 for the subsequent iterations. This redesign resulted in two separate but similar designs for the speaker: an acrylic speaker model and a 3D printed speaker model. Both speakers were tested with audio sweeps and scanning laser doppler vibrometer (SLDV) tests. After conducting these tests, both speakers were determined to be airtight and work as intended.

Acknowledgments

This project was made possible by many individuals other than those who directly worked on it. We would first like to thank our Advisor for the project, Professor Stabile, who guided us throughout the duration of the project. We would also like to thank the staff of the WPI Innovation Studio Makerspace, and the WPI MME Department without whom we would not have access to the necessary tools and working space to complete this project.

Table of Contents

Table of Figures

Executive Summary

In the speaker market today, commercial subwoofers are large and bulky which causes them to take up a lot of space or present themselves as obstacles. The objective of this Major Qualifying Project (MQP) was to design, manufacture, and improve a low-profile home speaker (LPHS) with the idea that it could fit in tight spaces such as behind a TV or under a car seat. The LPHS uses a moving magnet levered transducer (actuator) and passive radiators to give it a low resonant frequency while only being 2 inches thick. Previous MQPs which worked on this speaker were analyzed and iterated upon. While the main idea of the speaker actuation method was not changed from previous years, major design changes were made to the actuator and speaker box.

With the speaker box, the main goal was to create an airtight enclosure. This was achieved through two different designs. One was based heavily on the 2023 box, consisting of two, 3D printed halves split down the short length. Improvements were made to the method of sealing the two halves together and to how the active cone attached to the speaker. The second design was a more radical redesign utilizing laser-cut acrylic for much of the body. This design allowed us to use a silicone gasket to seal the box and it allowed faster iteration due to the speed of laser cutting. By keeping the speaker box airtight, we were able to use passive radiators to improve the resonance qualities of the speaker.

With the redesign of the speaker boxes, the active cones had to be redesigned and remade. Initially, a small change was made to the design of the outer plate which held the silicone surround, but this caused issues in the molding process. This was overcome with a second design which removed the outer plate during the molding process, leading to a much easier manufacturing process. The molding process for the silicone was improved and recorded.

The actuator design was also iterated upon to limit the amount of crashing that was occurring with the previous design. The actuator consisted of a base which connects to the speaker boxes and holds the stators, and the lever arm, which sits in the middle of the base and contains permanent magnets which cause the arm to move when the stators are charged. Multiple iterations of the base, stators, and lever arm were designed, manufactured, and tested. The largest changes were to the method of securing the stators and the lever arm to the base. An experiment was developed to test the force of the actuator.

Once the actuators for each speaker were assembled with the speaker boxes, testing and tuning was done using audio sweep tests and a scanning laser doppler vibrometer (SLDV). The audio tests were completed using a MATLAB program which swept through a range of frequencies and recorded the audio intensity observed by a microphone. The SLDV used a periodic chirp which ran through the same range of frequencies to quickly record the velocity response in the frequency domain of the entire active cone and passive radiator. By adding weights to the passive radiators and retesting the speakers, we were able to study the effect of passive radiators on the resonance of the speaker.

It was found that, without the passive radiators, the acrylic speaker had a single peak resonance at 58.75Hz, but once the passive radiators were added, a second, lower resonant frequency emerged, and the

initial peak resonance increased. As more weight was added to the passive radiators, both peaks of resonance were lowered.

1 Introduction

In this project our team was tasked with creating a low-profile subwoofer. Typically, subwoofers have large cones and feature big blocky enclosures. This can be a deterrent for consumers who do not have a lot of space or do not like the aesthetics of having a large speaker box in their home. A low-profile subwoofer with a small overall footprint could be stored behind a TV, behind or under a couch, or mounted on a wall. This allows for the more complete auditory experience that a subwoofer provides without the typical disadvantages of the average commercially available subwoofer.

As this was a recurring project, the team had a few previous prototypes of both the speaker box and the actuator to analyze as well as the documented experiences and advice of the previous teams through their papers. This information allowed the team to begin designing early in the project as many of the strengths and shortcomings of the previous designs were already known.

There were two main problems that needed to be solved in the project. The first was making the speaker enclosure airtight while still allowing the box to be taken apart and reassembled without affecting performance or threatening the integrity of the airtightness quality. Keeping the box airtight was important for incorporating passive radiators to improve the resonant properties of the speaker. The second goal was improving the design of the actuator to maintain the one-millimeter gap between the powerful magnets and the steel stators which, when lost, prevents the actuator from functioning and often requires the entire speaker to be disassembled.

2 Background

Speakers use electromagnets to move a diaphragm back and forth in a linear motion to create sound waves. On most loudspeakers, the electromagnet is connected to the diaphragm and is pushed and pulled from a permanent magnet below it (Figure 1). At lower frequencies, the diaphragm must move a significant amount to play at a significant volume. This means that bass speakers are generally very thick.

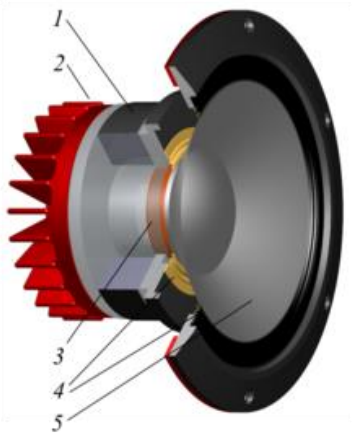

Figure 1: Design of a typical loudspeaker. The permanant magnet (1) sits behind the voice coil (3) which is connected to the cone (5). This Photo by Unknown Author is licensed under CC BY-SA

This MQP aims to solve this problem using a moving magnet levered transducer (MMLT), shown in Figure 2, to move the cone (Carlmark et al., 2012). With an MMLT, there are two permanent magnets held in a lever arm with opposite poles. These are pulled up and down by an electromagnet which sits in between the two permanent magnets and flips polarity due to the changing current of the audio signal. This arm is then connected to a diaphragm which moves the air around it, creating sound.

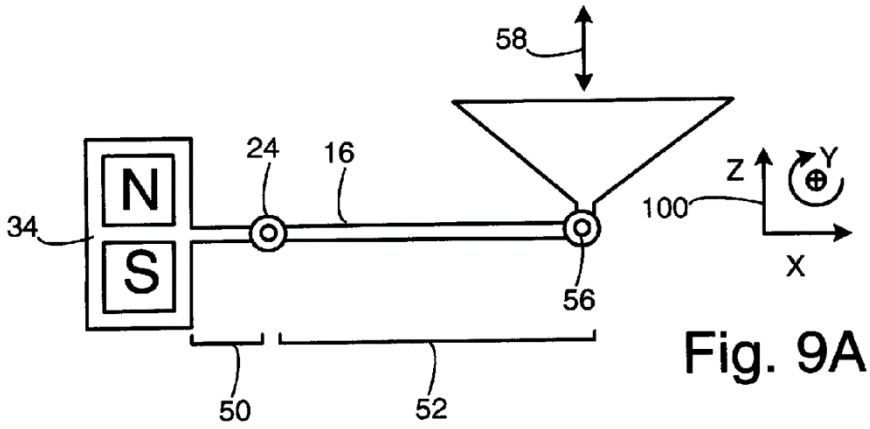

Figure 2: Diagram of moving magnet levered transducer (Carlmark et al., 2012).

With this design, the magnets do not need to move nearly as much to create the same range of motion in the diaphragm as a conventional speaker. The large amount of moving mass on the lever arm also means that the resonant frequency of this system is naturally already much lower. The extra mass and the mechanical advantage of the permanent magnets mean that much more force is required to accelerate the cone, meaning that the permanent magnets and the electromagnets need to be very strong.

Many bass speakers include horns or tuned tubes which are tubes that are open to the outside air. The shape and length of these horns can be used to tune the bass response of the speaker by changing the equivalent resistance of the air. These horns are usually fairly large and must go quite deep into the speaker, meaning that they are unsuitable for a low-profile system. Instead, we went with passive radiators. These are diaphragms with a tuned weight on them which resonates with the active cones due to changing air pressure within the speaker enclosure. These have a similar effect as the horns, but they allow the speaker to be much thinner.

By using both the MMLT and passive radiators, a speaker with a comparable frequency response to commercially available speakers can be made with a significantly thinner profile.

3 Evaluating Previous Work

The first part of the project was evaluating the work of previous MQPs. To create successful designs, it was important to understand the strengths and weaknesses of previous work done on this concept. We reviewed the reports on previous versions of this project, starting with the 2021 paper, which had insights on the initial design of the speaker box and actuator (Motler et al., 2021). The 2022 paper was helpful in the many appendices and instructions on molding the silicone surrounds and running tests (Zuber et al., 2022). Finally, we were able to directly analyze the prototypes and the report from the previous group to

understand many of the design choices that were made to improve upon previous years, and to study what we could improve (McLean et al., 2023).

3.1 Speaker Housing

One of the first things we did when we started this MQP was inspect the audio quality of the 2023 speaker. After this initial audio inspection, we suspected that the speaker housing was not airtight due to the lack of sound and vibration from the speaker cones and passive radiators. From this, we determined that our initial goal would be to make the 2023 speaker design (**Error! Reference source not found.**) airtight so t hat the passive radiators push out due to the pressure created from pressing in the active cones. If the enclosure is not airtight, the passive radiators will not move and therefore will not work.

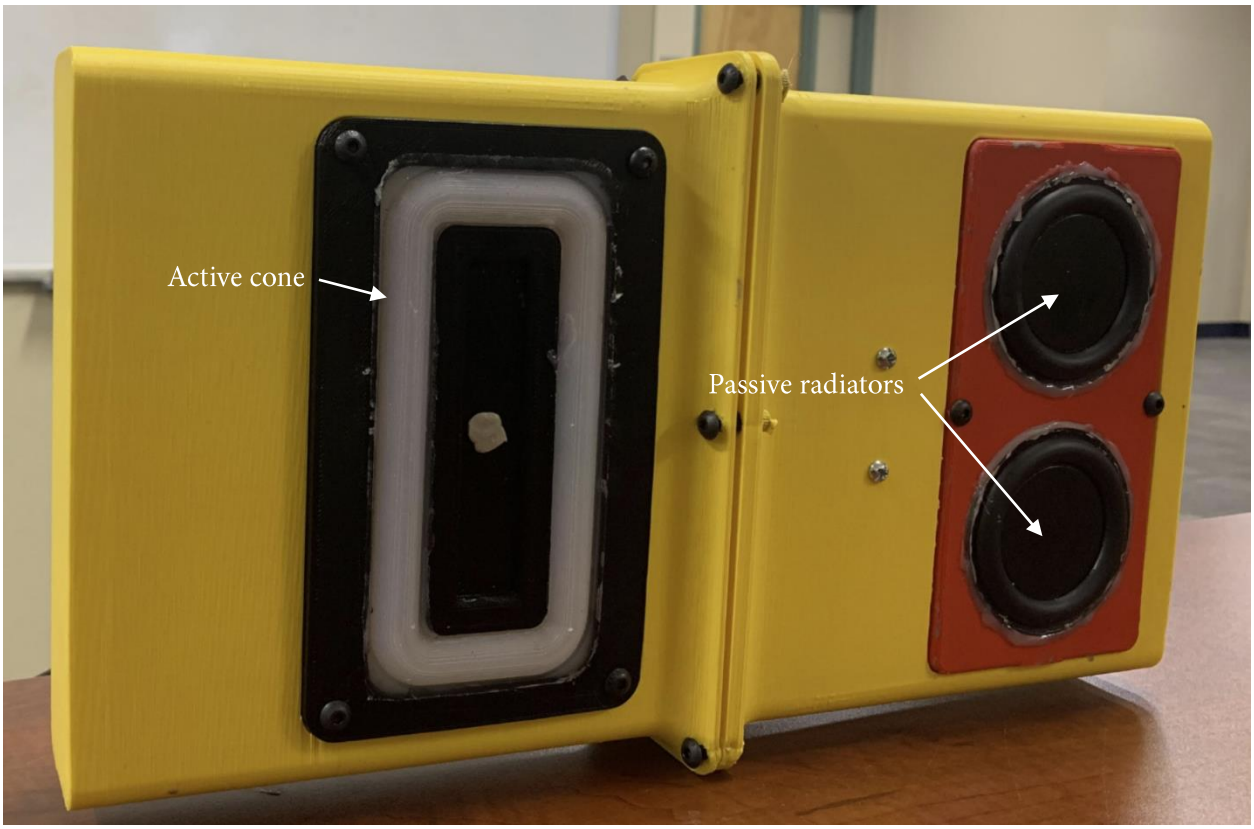

Figure 3: 2022-2023 final speaker prototype.

The first step in determining where air leaks occurred was to visually inspect the prototype and find areas of concern. We initially determined that the most likely places for leaks were at the interfaces where the 3D printed parts came into contact with each other as well as at the many screw holes throughout the body of the speaker. To get a better idea of the speaker assembly, we decided to take the speaker apart. Upon disassembly, we noticed that, while the 2023 MQP team used an O-ring in the middle where the two halves of the housing connected to keep their design airtight, it was difficult to tell if the O-ring was large enough for pressure to be applied to completely seal the connection. There were more O-rings between the speaker housing and the active cone and passive radiator plates. The O-rings were placed and secured by putty in a ridge that went around each rectangular mounting spot on the body, so like the first O-ring, we were unsure if there was any pressure being applied on the O-ring to seal the connection. Additionally,

there was a large amount of silicone caulk to assist with keeping the speaker airtight, however, we could tell that over time, the caulk did not hold together well, causing the speaker to lose its airtightness. Figure 4 shows the O-rings used at the central connection interface and one of the active cone mounting interfaces where putty can be seen holding the O-rings in place and silicone caulking can be seen around the flange. It can also be seen how the silicone caulking has peeled off over time and due to our team taking the speaker apart.

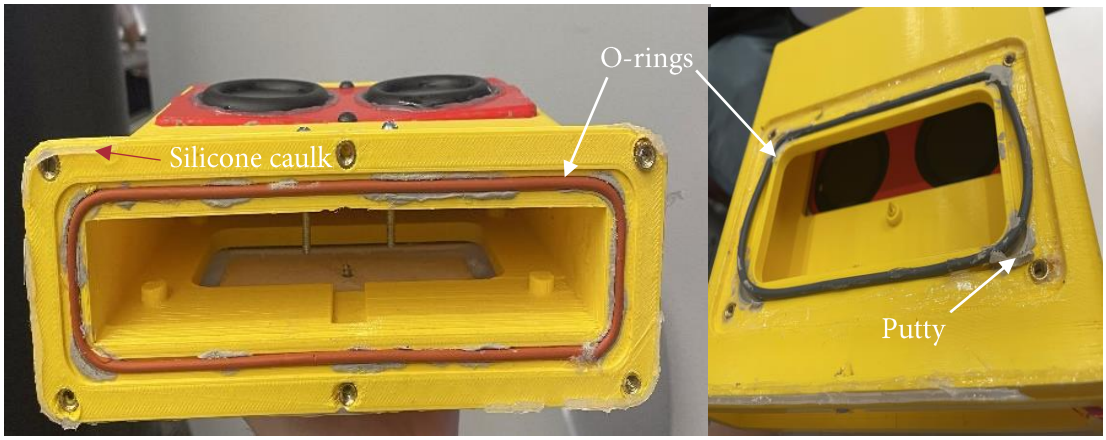

Figure 4: 2023 speaker O-rings and putty

After taking the speaker apart, we decided to rebuild half of the housing and check for air leaks by filling that half with water and finding where it poured out. We found that a significant amount of water leaked out of the interfaces between the 3D printed plates and the 3D printed body, as well as through the silicone caulk around the passive radiators (Figure 5). This showed that the O-rings under each of the plates were not keeping the connection airtight. This test did not test the interface between the two halves of the main printed body. However, as the O-rings used in other parts of the design did not seem to work well, we expected that this interface would not have created a decent seal.

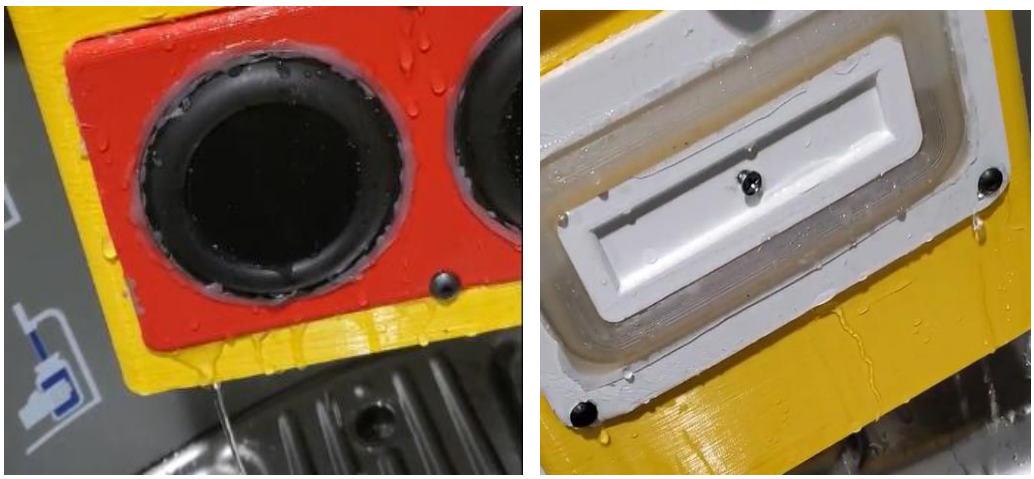

Figure 5: Water leaking from 2023 speaker from water test

The previous design had some other issues to address that potentially affected the airtightness. One issue was that the previous team used threaded heat inserts that were not properly placed at the correct angle, which caused alignment issues between the holes on the two halves of the speaker box. Also, the active cone plates were mounted with four screws in the corners and the passive radiator plates were mounted with only two screws. We suspected that there were not enough screws to apply an even amount of pressure around the plates to keep them sealed especially since thin PLA plates bend easily. Additionally, the screws were placed too close to the edges of the plates, causing them to crack.

Another problem was that the wires that connected to the actuator inside the speaker box were inserted through a hole which was sealed with putty. This didn't seem like a method of sealing that would be effective long-term. Putty was also used to seal up the extra set of actuator base mounting holes. There is a set of these holes on each half of the speaker box, but when installing the actuator, only one set of the holes was used to secure the actuator, so it left the other set of holes in need of being sealed. However, like with the hole for the wires, the putty did not prove to be the best method of sealing it up.

Figure 6: Putty sealing holes for actuator wires and unused actuator mounting holes

3.2 Actuator

When evaluating the actuator, the main issue was that it was “crashing”. This means the gap between the magnets and the stators, which needs to be maintained at one millimeter for the actuator to function, had been lost which locks up the actuator and prevents functioning. This was happening through a combination of the magnets sliding out of the arm and the stators sliding out of the base. Upon inspection, it appeared that the magnets were held into place using hot glue which did not properly secure the magnets even though the slot was a tight press fit. The stators were held down using a printed bracket that was thick but was still bending across the stators due to tolerancing issues and the limited stiffness of PLA.

Figure 7: 2023 Actuator

In addition to these issues, Professor Stabile requested that the actuator be made more robust overall, and that the method of attachment for the pin be changed to a “V” shaped slot, as opposed to the original cylindrical slot with a “V” cut at the top. The actuator could be made more robust by changing the layout of the actuator base and attachment method to the speaker box as the previous design had some complex geometry that was weak when printed. Due to the crashed actuator, and the previously mentioned issues with the speaker box, we were unable to do any testing on the actuator or the speaker.

4 Methodology

4.1 Design

The design of this project was primarily based on the work of previous groups who have worked on this project. The designs from 2022 and 2023 were studied and improvements were made to increase the robustness of the actuator and make the speaker boxes airtight.

When beginning design work, the team did not want to disregard the successes of the designs of previous years and opted to largely build upon previous designs, mostly making improvements in areas where they fell short. With the two main goals of the project being an airtight box and a more robust actuator, the following redesigns were made.

4.1.1 Actuator Design Modifications

When making changes to the actuator, some considerations were taken to preserve the design concept, and the function. The previous design was measured and the scale of the base and the arm relative to each other and the rest of the speaker remained the same. Additionally, the location of the mounting holes on the base were kept the same to allow for the actuator to be a suitable replacement with the same design principles. This also prevented major changes from being needed on the boxes to accommodate the actuator. Additionally, important hardware such as magnets, bearings and pins were carried over to the new designs.

Base

The first change to the base was the shape of the pin slot. The original pin slid through the slot which was a tight fit but inconvenient to assemble and disassemble. This was changed to a "V" shaped slot which simply centers the pin.

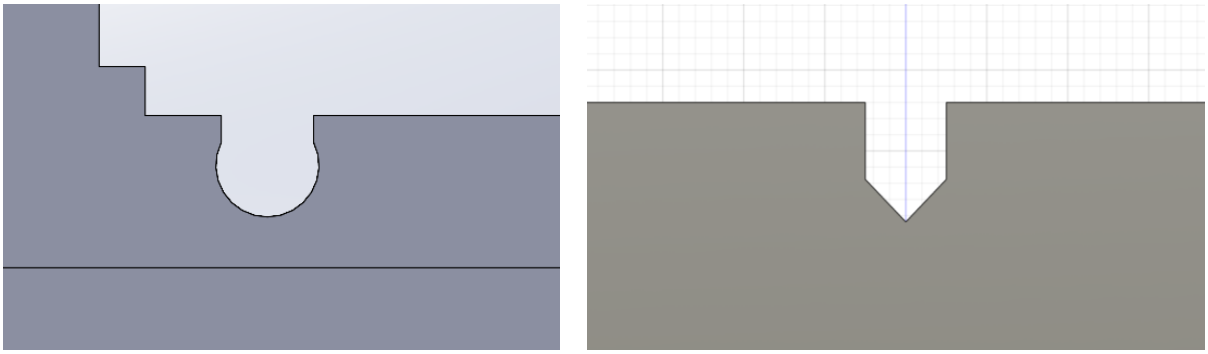

Figure 8: Slot that the pin sits in. 2023 design (left) and initial 2024 design (right).

An M4 threaded heat insert was installed and an M4 bolt and 20mm diameter washer were used to apply pressure on the pin, which sits slightly proud of the slot, holding it tightly in place.

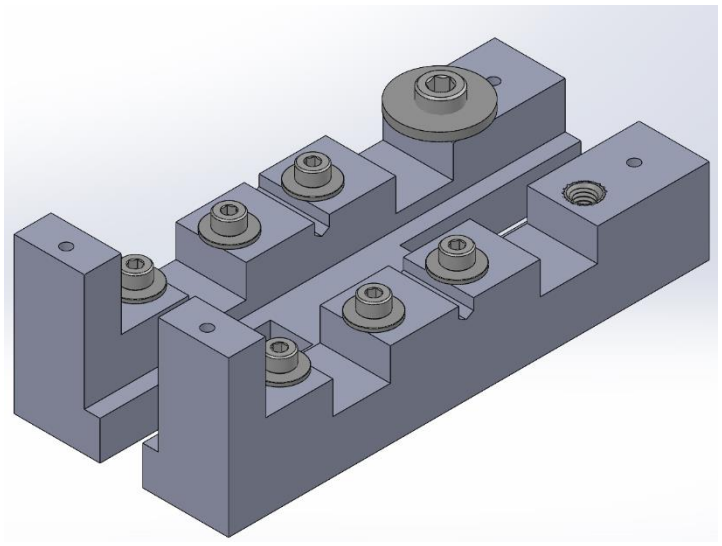

Figure 9: First iteration of actuator with hardware.

This required one side of the pin slot to be lower than the other causing one side of the stator to be less supported. This was compensated for by using an M6 bolt and washer to hold the stator on the thinner side. The first iteration of the base also included a new method to attach the actuator to the box. The previous design's arms were replaced with a simpler and stronger raised section with threaded inserts. The pin slot was moved to be geometrically centered in the base by making the top attachment points taller, but this allowed for excess material to be removed from the bottom of the base which resulted in a net slimmer base, allowing the boxes to be thinner as well. The lever arm geometry was later changed to adapt to this by being made symmetrical which simplified how the actuator functions and helped ensure the cones would be moved evenly.

Final Iteration

With this final base design, the main goal was to improve the pressure applied to the stators and to improve manufacturability. Since the previous iterations applied pressure to the stators through a washer screwed into the base from the side, much of the force of the screw is being applied into the base rather than the stator. Another issue that was solved with this iteration was to remove the heat set inserts as we were dissatisfied with the tolerances we could get with them.

To fix these problems, we decided to move to a design with bolts that go through a slot in the stator. This allowed us to tighten the stators in place with much higher force without worrying about the heat set inserts getting pulled out of the 3D printed base. To not affect the magnetic flux of the stator, the cross-sectional area of the stator was kept constant by adding a bulge around the slots on the stator that the bolts go through.

Since we changed the design of the stator, one of the few custom metal parts on the speaker, we had to figure out how to manufacture the new stators. None of the members of this MQP team had any experience machining steel, so it was decided to use a laser cutting service called SendCutSend. With this service, we sent in a .dxf file with the profile of the stator, and it was cut out of 0.375", low carbon steel. Each of the stators cost only about $8 which was well worth not machining the parts ourselves.

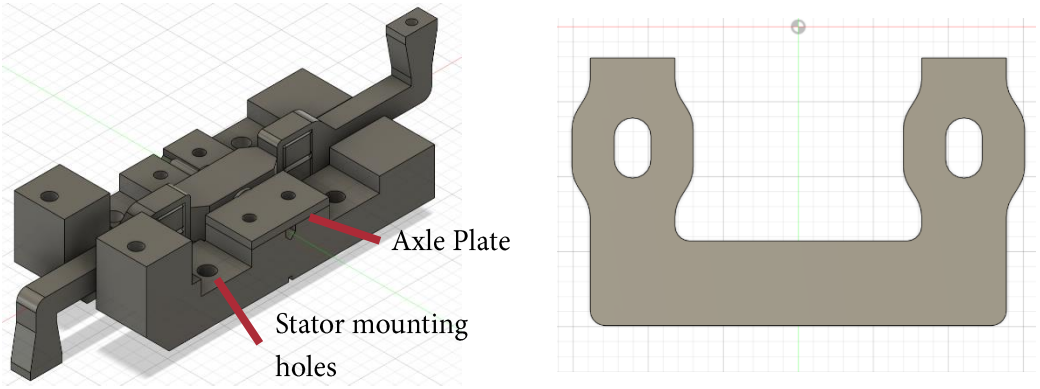

Figure 10: Final base and lever arm design (left) and stator (right).

As we were preparing an order from SendCutSend, we decided to design custom plates to hold the axle on the arm rather than the washers used in the previous iteration. The rectangular plate created a larger contact area between the axle and the plate, creating more friction to hold the axle in place. The rectangular plates also had bolts on either side of the axle rather than the washers, which cannot provide as much pressure due to the offset between the bolt and the contact point.

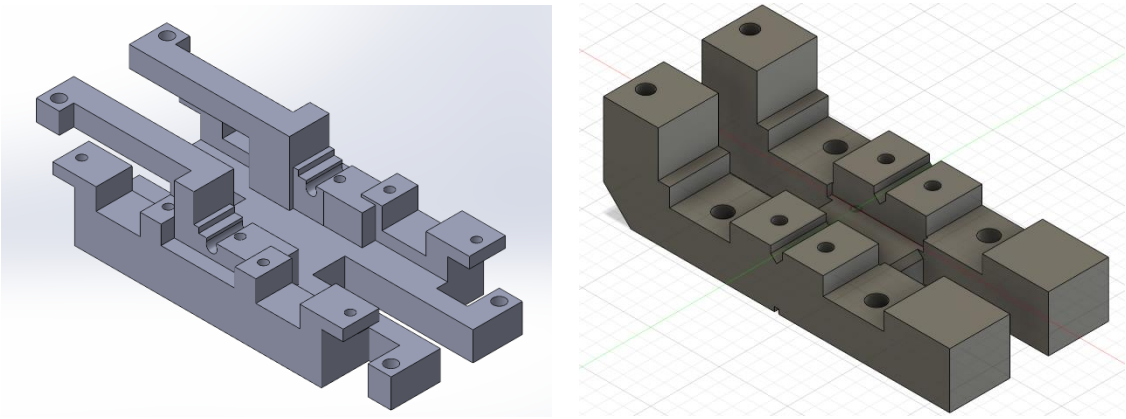

Figure 11: Original base (Left) and final base (Right)

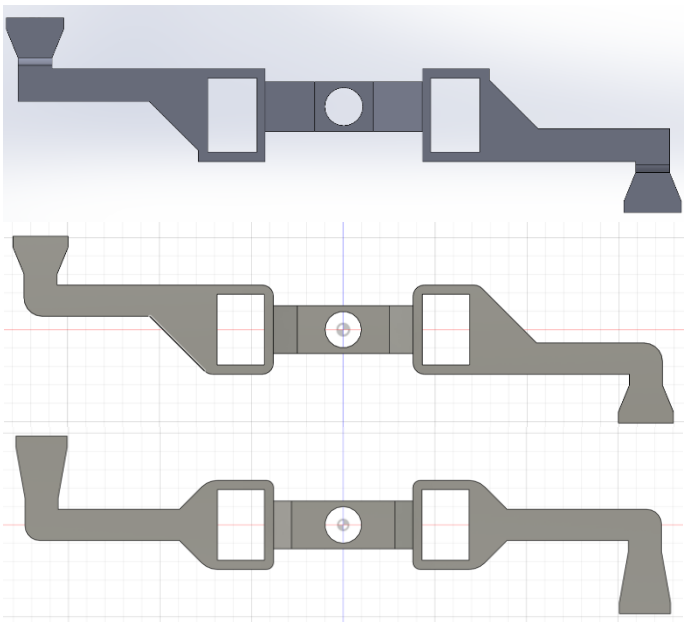

Figure 12: Original lever arm, first iteration, and final lever arm (top to bottom).

Lever Arm

When analyzing the previous year's lever arm, it was determined that the top of the magnet slot would be made slightly thicker to help with rigidity and the magnets would be held in place with superglue to fix the main issue of the arm which was the magnets sliding out of place. In addition, the geometry of the arm was adjusted to better fit the updated base as mentioned previously. The comparison between the two designs can be seen above. The new arm design is symmetrical, and the vertical portion of the arms are a bit longer to accomplish the same travel as the previous design. The corners were filleted to help with printing. The changes allowed for a more low-profile design and improved the alignment of the magnets and the stators while maintaining the necessary travel for the speaker to function.

The only other change made to the arm was the method of preloading the bearings. The original method consisted of two small 3D printed rings that slid onto the pin and sat between the bearing and the base, preventing the arm from sliding and putting some force on the inner race of the bearing. This method did not properly preload the bearing.

The first new iteration of the actuator assembly added a spring between the two bearings. The spring pushes out on the inner races of both bearings, preloading them as the outer races are glued to the hole in the lever arm. An approximation of this can be seen in Figure 12.

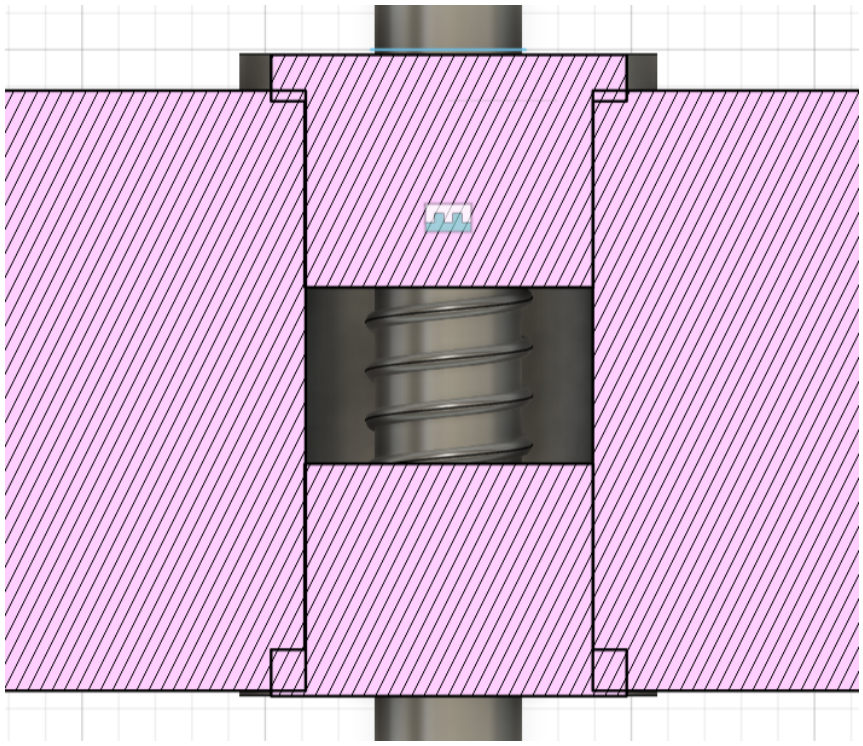

Figure 13: Preloading bearings with a spring.

The final design eliminated the need for the spring by gluing the inner race of the bearings to the pin, preloading them during gluing. This was done gluing the outer race of the bearings into the slot of the arm and then sliding the pin through both bearings. The inner race of one bearing is glued to the pin and set to dry fully. Then the inner race of the second bearing is glued to the pin while applying pressure to the pin, preloading both bearings. This method eliminated almost all unwanted side to side play in the bearings and prevented the arm from sliding laterally on the pin.

4.1.2 Active Cone

One of the largest issues we faced when producing new speaker prototypes was manufacturing the active cones. As we made significant changes to the shape of our active cones from the previous year's cones, it made more sense to model and mold entirely new cones than to work with the cones that had been designed previously.

Iteration 1

The first iteration of the new cone design was only a slight modification of the previous year's design. Their active cone consisted of three parts: a 3D printed outer plate, a silicone surround, and a 3D printed diaphragm in the center (Figure 14, top). To make one of these, the 3D printed parts were placed into a 3D printed mold and then silicone was poured in which would then set and hold the two halves together. We decided to initially keep this general idea and make some small modifications such as adding a flange on

the outer piece to facilitate better alignment when assembling as well as adding two more screw holes to provide more pressure on the gasket which would keep the speaker airtight.

The biggest problem with this design was tolerancing. The flanges meant we needed to add a slot in one half of the mold which needed to be large enough for the flange to fit in, but small enough that it did not move around too much and ruin the cone. After a few failed attempts at getting the tolerances right, we decided to move on to Iteration 2.

Iteration 2

In this second iteration, we made some larger redesigns. The biggest change we made was that we got rid of the need for the outer plate during the mold. Since the speaker cone was molded out of silicone, we determined that it could also be used as the gasket. This meant that we would only have to mold the surround and 3D printed diaphragm together and we could remove the need for a laser cut gasket entirely. This iteration was extremely successful and allowed us to make functional prototypes.

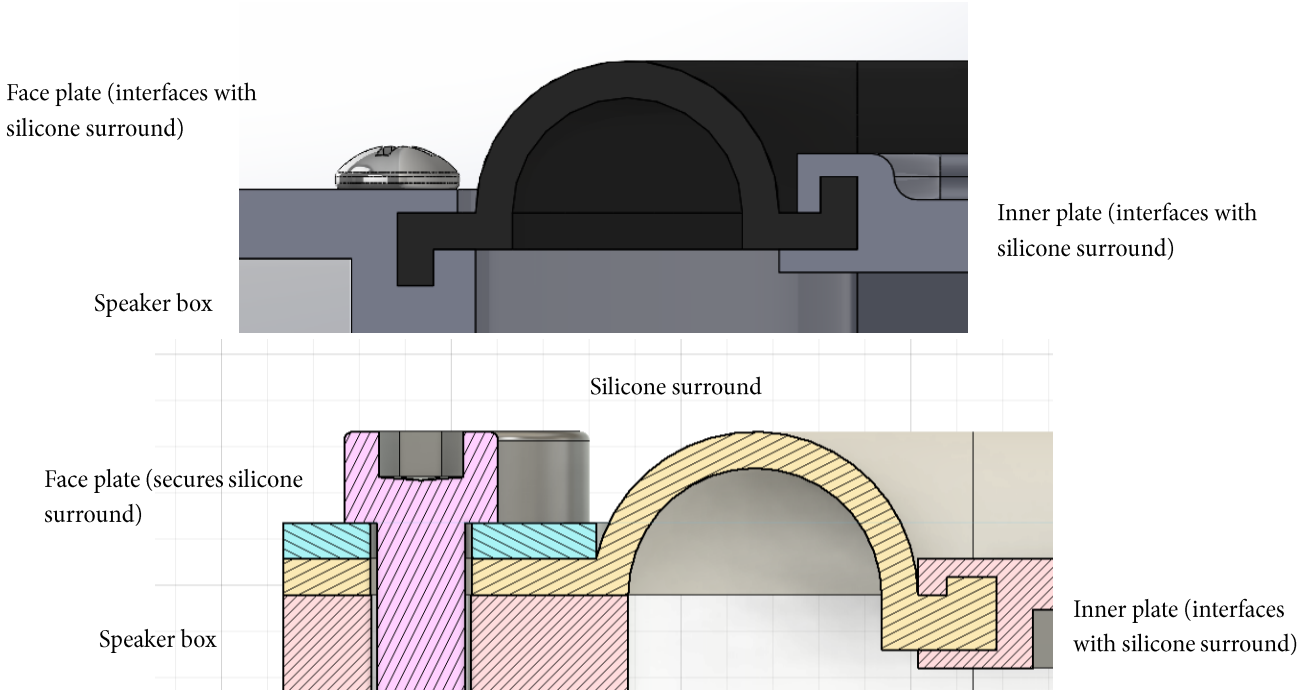

Figure 14: Cross section view of active speaker cone. Iteration 1 (top) has the 3D printed surround that the silicone locks into. Iteration 2 (bottom) does not flow into an outer plate.

4.1.3 Speaker Case Redesign

After assessing the state of the previous speaker housing, we brainstormed ways to improve upon the previous design. To improve airtightness, we decided to change from O-rings to laser-cut silicone rubber gaskets. Using gaskets rather than O-rings allows us to laser cut them in custom-designed shapes to fit wherever we want. We also decided to add dual banana sockets with a gasket underneath to the case instead of having a simple hole. This allowed us to have a more airtight seal for the electrical connection.

As we were conducting our initial ideation, we decided that we wanted to investigate two different design options when redesigning the case. One was based much more off the previous design. It would be mainly 3D printed, so we called it the "3D Printed Design." The other design was a much more significant redesign because it was mainly made of laser cut acrylic rather than a fully 3D printed box, so we called it the "Acrylic Design."

3D Printed Design

While there were some issues with the old design, there were many design choices which we found beneficial. One design choice we made for this design was splitting the case in half along the shorter axis. This was beneficial because there was less surface area to seal when trying to make the case airtight. Like the 2023 design, this case was also designed to be printed as only two parts. Even though these parts would take a long time to print, it would be inexpensive and would not require much supervised manufacturing time. This design ended up going through a few iterations.

Iteration 1

The first iteration modified the previous year's speaker housing by changing the dimensions to make the overall housing smaller, making the flange where the housing is split larger for better clamping, and adjusting the mounting features to accommodate the change in the mounting method for the cones and passive radiators. This iteration can be seen in Figure 15.

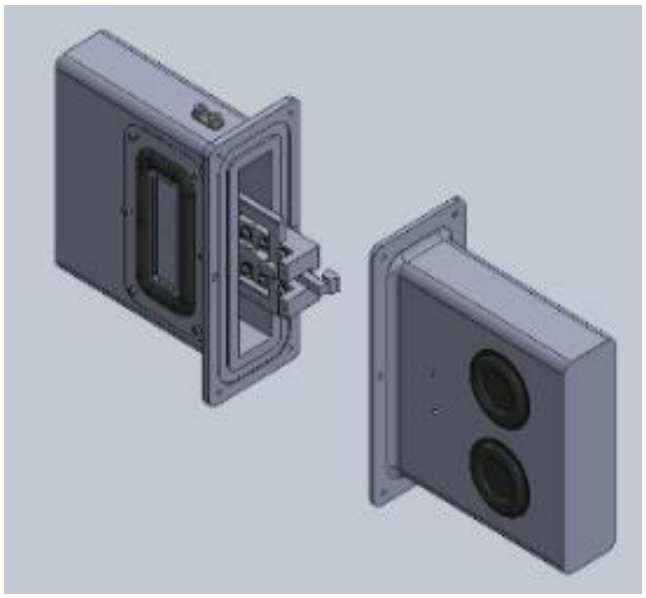

Figure 15: Iteration 1 full assembly in SolidWorks

With this initial iteration, the speaker box is slightly thinner than the 2023 design, and the flange is larger. More significantly, the passive radiators are mounted directly onto the housing over circular holes rather than being attached to a plate that is then mounted onto the housing. Additionally, the cone plates have mounting holes at the midpoints of the long sides of the plates in addition to the four holes in the corners to help create a better seal around the plates. The cones also each have a gasket made of silicone rubber that would be laser cut to fit perfectly in the mounting spots on the speaker housing. Lastly, instead of just

a simple hole to insert the wires of the actuator through, the holes on the side of the speaker were designed so that a banana plug, along with its own gasket made of the same silicone rubber material, could be installed.

Iteration 2

The biggest change made for the second iteration involved changing the method of connecting the two halves of the housing. This iteration no longer has a flange through which bolts are used to clamp the halves together. Instead, the following highlighted profile sketch was swept cut around one half of the housing:

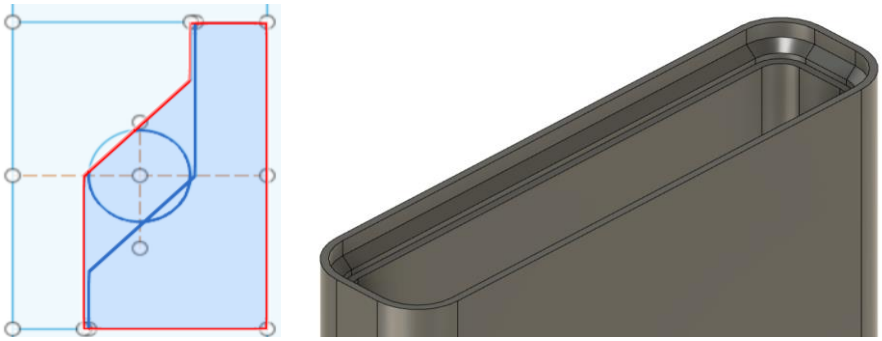

Figure 16: Profile sketch and sweep cut for top side in Fusion 360

On the other half of the housing, the following highlighted profile sketch was swept cut:

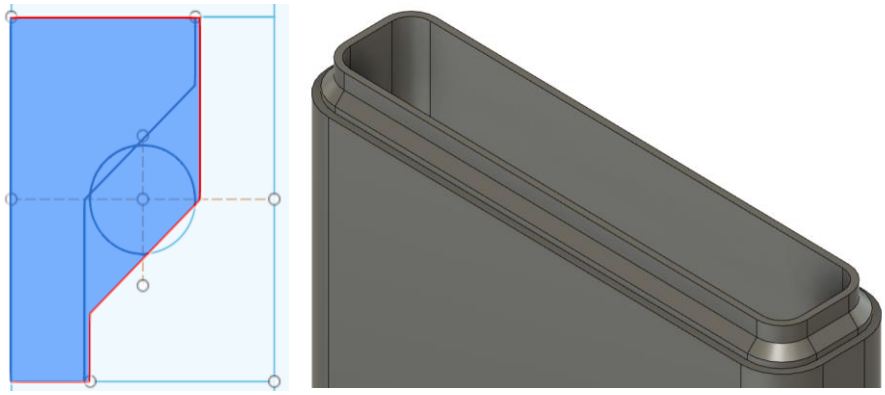

Figure 17: Profile sketch and sweep cut for bottom side in Fusion 360

These sweep cuts allow the two halves of the housing to fit nicely together while applying some pressure onto a rubber O-ring in-between to create a tight seal and so that the outer surface is flush allowing the overall speaker box to be more low-profile (Figure 19).

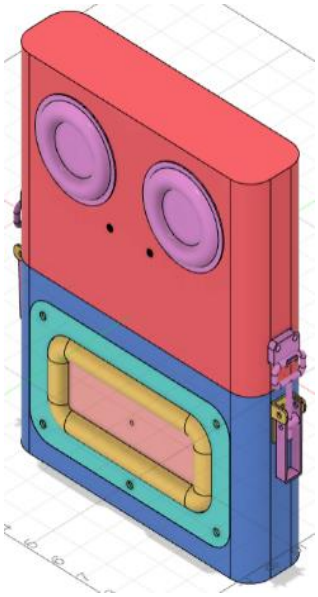

Figure 18: Full 3D printed speaker box assembly in fusion 360

As seen in Figure 18, there are clasps on the sides of the speaker box that are meant to tightly clamp the two halves of the speaker box together. With the pressure from the clamps holding the two halves of the speaker box together, the O-ring in-between creates a nice seal. Additionally, the speaker was made a little shorter to make the overall speaker smaller, thus more low-profile. As seen in the exploded view, the speaker was also designed to have the silicone active cone act as the gasket between the cone plate and the body of the speaker rather than using the laser-cut silicone rubber gaskets, as explained in Iteration 2 of section 4.1.2.

After this iteration of the CAD design was completed, the speaker was manufactured and assembled.

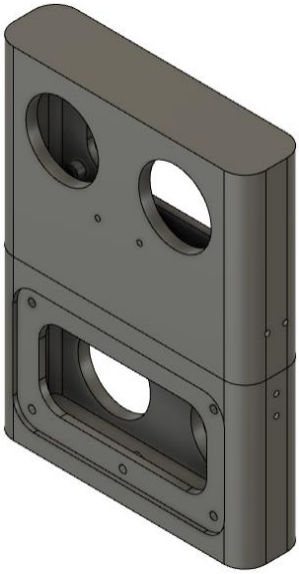

Figure 19: 3D printed speaker box in Fusion 360.

Iteration 3

After the speaker was assembled, we noticed that the cone plates bulged a little on the side where there wasn't a screw at the midpoint. Additionally, over time, we noticed that the cone plates were starting to crack where the screws were and some of the heat set inserts were starting to be pulled out. These issues threatened the quality of the airtightness of the speaker box, so the third iteration saw some modifications to the design that helped to improve the airtightness. One modification was adding two holes equally spaced apart along the side of the cone plates that did not have a hole at the midpoint (Figure 19) as a midpoint hole would interfere with the actuator arm. Additionally, the cone mounting spot on the speaker housing was enlarged a little, which can be seen in the full assembly model (Figure 20), to allow some room for the silicone to push outward from the pressure of the cone plate. The purpose of making these two modifications was to help get rid of the bulge while not interfering with the actuator on the inside of the speaker.

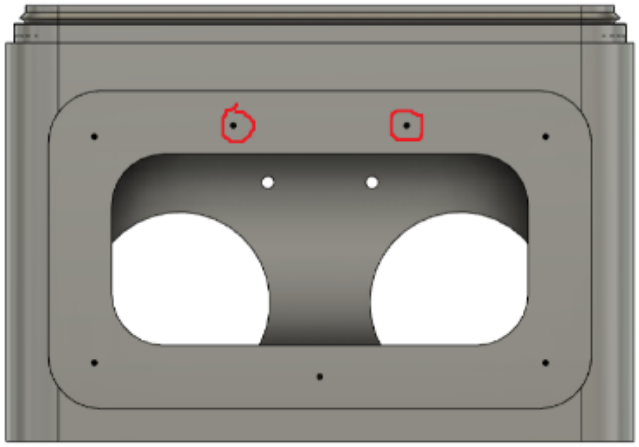

Figure 20: Bottom side with two new mounting holes for active cones.

Figure 21: Final 3D printed speaker full assembly

Acrylic Design

While working on the 3D printed design, we also worked on a more radical redesign which incorporated laser cut acrylic plates to construct most of the box. The goal of the acrylic plates was to reduce manufacturing and assembly time, increase precision on the parts we used, and to have smoother surfaces to allow for better sealing. With the 3D printed case, each half of the case required print times exceeding 20 hours with very fast print settings, leading to poor tolerances. The assembly of the box was also an issue as it had many axes of assembly and required reaching deep into the box to connect wires. The layer lines of the 3D print also made creating a seal more difficult. In contrast, the acrylic design required significantly less printing time, the laser cut acrylic face plates could be manufactured quickly, and the flat surface of the acrylic were better for creating an airtight seal.

Iteration 1

The acrylic design consisted of two laser-cut acrylic plates on a 3D printed frame with silicone gaskets between the plates and the frame (Figure 22). This iteration aimed to be a similar size to the speaker produced by the previous team. It used thread forming screws for plastic (plastites) to fasten most of the components together as these could be directly screwed into the 3D printed plastic and the acrylic face plate rather than requiring the installation of heat set inserts.

Figure 22: CAD of iteration 1.

While this iteration seemed easier to manufacture, the frame still had to be printed in two pieces to fit into the available print bed, which could cause some issues with air leakage at the seam. To combat this, bolts were used for securing the two halves together with sufficient force, and a slot was created to hold a length of O-ring cord stock.

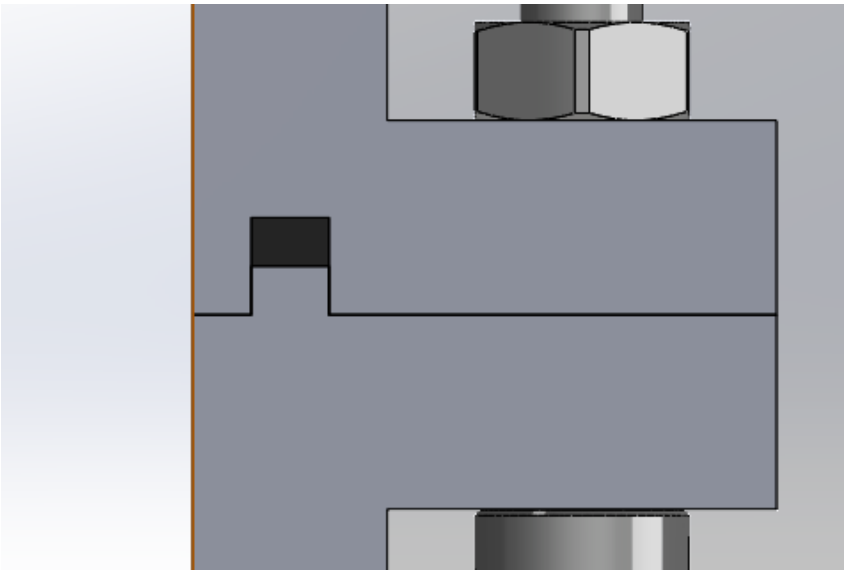

Figure 23: Close up view of the connection between the two 3D printed surround pieces with a slot for O-ring chord stock.

This iteration was never fully assembled as it was designed to use the failed iteration 1 active cone, which meant that we could not test whether it was truly airtight. With the issues found during assembly, we were quite sure that the seal on the box would not be sufficient. With the knowledge of the issues with this prototype, we moved onto the next iteration of the acrylic design.

Iteration 2

In iteration 2 of the acrylic design, we looked to fix many of the issues that we had with the first iteration. One of the biggest issues that was addressed with this redesign was the use of plastites. These were replaced

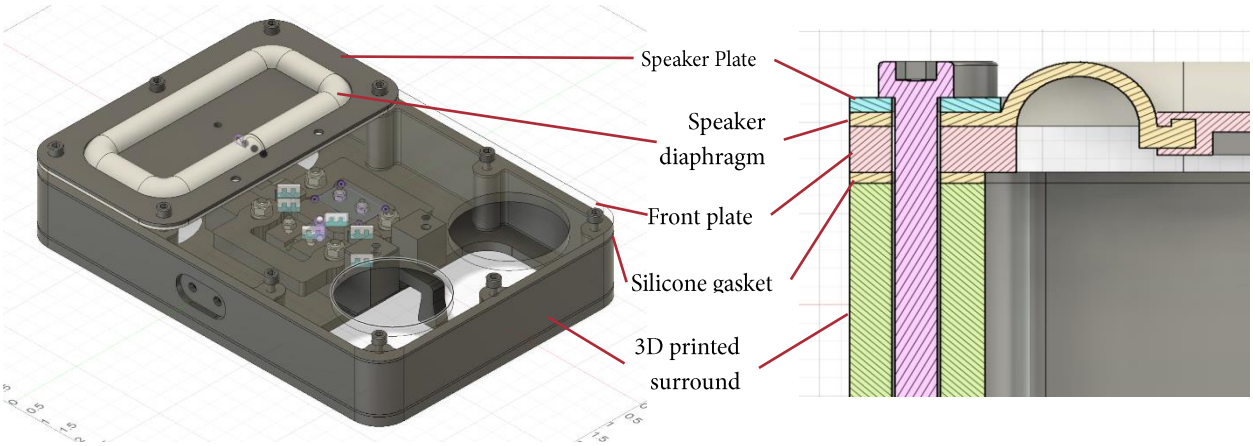

Figure 24: CAD assembly of iteration 2 acrylic design (left) and cross section of the interface between the active cone and the speaker box (right).

with through bolts. We also shrunk the case so that the screws which held the case together also held the active cone onto the case. Shrinking the case also had the added benefit of allowing us to print the outer frame as one piece rather than two, eliminating any interfaces between two 3D printed pieces. Due to the poor tolerances of 3D prints, interfaces between two printed parts would likely have issues with airtightness.

The flat surface of the acrylic plates allowed for the use of super glue to fasten the passive radiators to the face plate as well as giving us the ability to easily change out the face plate. This was useful in creating a test box without the passive radiators to study the effect that they had.

This iteration proved to be quite airtight and was successfully used as a test platform for studying the effects of the weight of the passive radiator.

4.2 Manufacturing

4.2.1 Active Cone

To mold active cones for our speaker prototypes, we first needed to create a mold. We did this by 3D printing two parts which, when placed together, matched the negative space that surrounded the active cones in the models of the speakers. Within these two halves we inserted liquid silicone, which, after solidifying, formed a new active cone. The newly produced cone could then be removed from the mold to repeat the process and create additional cones. To improve the quality of the speaker cone with each molding attempt, we tweaked variables such as the pot life of the silicone parts and the length of time to run the vacuum chamber, which resulted in each speaker cone made being superior to the previous one.

4.2.2 Speaker Box Housing

3D Printed

Iteration 2

The first iteration of CAD for the speaker box was never printed. The second iteration CAD design of the speaker box for the 3D printed design was printed on an Ender 3 V2 with a 0.8 mm nozzle. By using the 0.8 mm nozzle rather than the standard 0.4 mm nozzle which comes with the printer, we were able to increase the layer height from 0.24 mm to 0.48 mm. This significantly decreased the printing time of the two halves. With the standard nozzle, the print was projected to take about 40 hours, while the 0.8 mm nozzle brought the print time down to about 18 hours. These print times are still quite large, and the larger nozzle reduces the accuracy of the print, making finer details impossible to make.

With Iteration 2, the box halves were printed with 2 walls (1.6 mm) and 10% infill. These thin walls, plus the distortion caused by using the large nozzle, created oval-shaped holes where the heat set inserts were supposed to be pressed in. This led to inaccuracies in their placement as well as reducing their strength, causing some to be pulled loose after repeated use.

The cones were made of silicone as explained in section 4.2.1 above. M5 threaded heat set inserts were placed in each of the cone mounting holes so that the cones and cone plates could be mounted. M3 heat

set inserts were placed in the holes for mounting the clasps. The passive radiators were stuck on using a silicone sealant.

Figure 25: Completed iteration 2 3D printed speaker.

Iteration 3

The print settings were changed slightly when printing the 3D printed design for the second time. Four walls (3.2 mm) were used rather than two used previously, and the infill was increased to 20%. By using these settings, we were able to use the small pilot holes to drill them out for the heat set inserts rather than rely on the oval-shaped printed holes. This allowed for more accurate positioning, hole size, and a stronger bond with the heat sets.

For this iteration of the speaker's manufacturing, we had the cone plates manufactured out of 6061 T6 aluminum by SendCutSend. Having the plates made of aluminum helped to make them stronger so that they didn't crack at the holes from the pressure of the screws. Since the active cone mounting holes were more uniform from drilling them out, we were able to more accurately place the M5 heat set inserts, which made installing the cones easier and prevented the screws and heat set inserts from being installed at an angle which ruins the threads. The passive radiators from the first physical iteration speaker were carefully removed and stuck onto the new iteration 3D speaker box with the same silicone sealant.

While the cone mounting holes in CAD were made into pilot holes to drill out, the holes for mounting the clasps were not changed, so we drilled out the holes on the clasps and clasp hooks to make them uniformly circular like the cone mounting holes. This caused us to have to size up to M4 heat set inserts instead of the M3 ones from the first 3D printed speaker but improved the rigidity of the clasps.

Figure 26: Fully assembled 3D printed speaker

Acrylic

Iteration 1

This iteration proved the manufacturability of the acrylic design. It was easy to produce, requiring two, eight hour prints as well as about an hour at the laser cutter to cut out the acrylic face plates and silicone gaskets. One clear benefit to this design was that both face plates and the gaskets made for the plates were identical. This meant that the same setup could be used many times to create the face plates.

During the cutting process, the acrylic cut very cleanly, but the silicone burned at the edges, leading to an ash buildup that needed to be cleaned off. It was noted that the cutting head of the WPI laser cutter was not properly aligned to the print bed, leading to slanted cuts in the acrylic. This did not cause any issues during assembly as the tolerances designed into the box were sufficient to make up for the inaccuracies in the laser cutter.

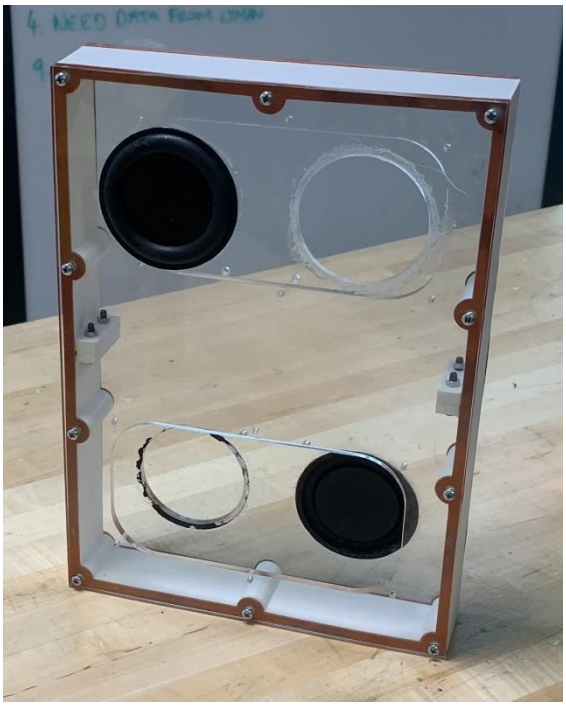

Figure 27: Iteration 1 acrylic speaker. This was never fully assembled as it used iteration 1 active cones.

This iteration did show some issues which would need to be overcome in future iterations. One main issue we found was that, due to inaccuracies in the WPI Makerspace 3D printers, the two printed pieces were significantly warped at the corners, causing there to be gaps between the printed case and the acrylic face plates which were too large for the gasket to fill. We also found that the plastites used to hold the box together could not provide sufficient pressure before stripping out the holes they were screwed into.

Iteration 2

With the second iteration, the acrylic plates were much smaller, allowing us to use smaller pieces of stock when laser cutting. The 3D printed frame was also much faster to print and could be printed as a single part on a WPI Makerspace Lulzbot TAZ printer. One corner was still warped, but due to using bolts rather than plastites, a greater force could be applied to the acrylic plates, conforming them to press onto the silicone gasket material.

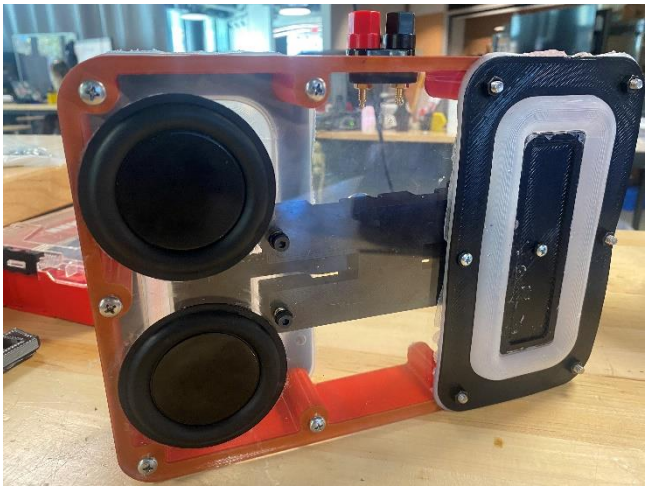

Figure 28: Iteration 2 acrylic speaker design fully manufactured and assembled with actuator.

Once this prototype was assembled, we found that the 3D printed speaker plates were not strong enough and were bending and cracking, just like the 3D printed design. These were replaced with 2mm aluminum plates which were ordered through SendCutSend.

4.3 Actuator

The actuator was initially printed out of PLA using the WPI makerspace's Ultimaker 3 printers. The first few attempts at printing the actuator were unsuccessful due to quality issues with the makerspace printers. This led us to use Professor Stabile's Ender 3 printers instead, which could use Ultimaker Cura to slice the parts. Cura gives much more control over the print settings than 3DPrinterOs, the software used by the WPI Makerspace. This greatly improved the print quality of the actuator and base. Once all parts were printed, the bearings and magnets were inserted into the lever arm. A Hall Effect sensor was used to check the polarity of the magnets before they were pressed into the slots on the arm using a vice. The stators were wrapped with approximately 250 turns or 45 ft of wire each. This was done by attaching the stator to a motor using a 3D printed mount and spinning it while feeding the wire.

4.4 Testing

Three tests were conducted to determine the quality of the speakers. The first test was the actuator strain gauge test. This was conducted to determine the force that the actuator arm could produce. The second test used a scanning laser doppler vibrometer (SLDV) to obtain precise vibrational characteristics of the active cone and the passive radiators. The final tests were audio and sweep tests, which were used to determine the quality of the sound that was produced by the speakers.

4.4.1 Actuator Strain Gauge

One test we had to complete was strain gauge testing. With these tests, we used a strain gauge to measure the force that the actuator arm applied at various voltages. Last year's group used a constant power supply of 20V and a rheostat to control the voltage of the actuator arm. They measured the force applied to the strain gauge over time as they swept through the rheostat. This method was able to measure the maximum force applied at 20V, but it did not measure the voltage or current going through the stator. We did attempt to use this technique to test our actuator, but we decided to change the test to record the voltage and current.

To obtain the relationship between force, voltage, and current, we used a DC power supply. With this, we were able to test the force at voltages between 0 and 12 volts at 0.5V increments. At each voltage, the current was measured using the power supply, which displayed the current as voltage was applied. These were then plotted in excel to observe the characteristics of the actuator arm.

4.4.2 SLDV

A scanning laser doppler vibrometer (SLDV) was used to identify the resonant frequencies of the speaker test boxes. An SLDV is a device that can measure the vibrational velocity of an object using the doppler effect. A 670 nm, coherent laser source is passed through a beam splitter into a beam that goes to the object (the object beam) and a beam that goes through a Bragg cell to alter the frequency (the reference beam). The SLDV combines the object beam and the reference beam and observes the beat frequency. When the object beam is reflected off the object, if the surface is moving, the reflected frequency is altered slightly, changing the beat frequency. This change can be translated into the velocity of the surface. By sweeping through frequencies, a full spectrum frequency response can be recorded.

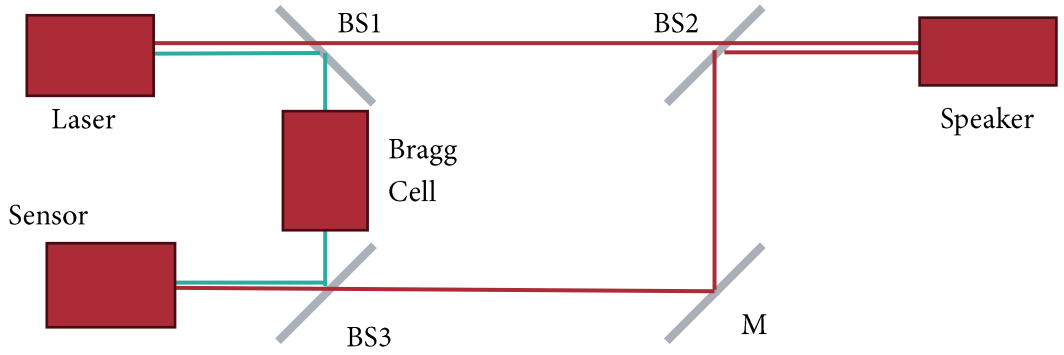

Figure 29: Diagram of an SLDV. BS are beam splitters and M is a mirror.

We used a Polytec PSV-400 scanning head which uses a 670 nm red laser. This was set up on a tripod with adjustable height and angle. The speakers were held in a vice about 6 feet away from the scanning head on an optical table.

To set up the scans, a 2D alignment was performed at the four corners of the box and various points on the speaker cone and passive radiators. Then, the scanning points were defined at both the active cones and the passive radiators. A periodic chirp was used to sweep through frequencies from 10Hz to 500Hz and a FFT was used to obtain the frequency magnitude response of both the active and passive cones. Issues

were encountered during testing, causing the tests to use different amplitudes in the amplifier, therefore, to compare the different tests, the frequency response data was normalized by dividing the recorded amplitudes by the maximum recorded amplitude. Metal weights were added to the passive radiators on the acrylic speaker to test the effect of mass on the resonant frequency.

4.4.3 Audio and Sweep

Audio Test

For both the acrylic and 3D printed speakers, we conducted qualitative audio tests to determine what frequencies each of the active speakers and passive radiators resonated at and where on the speaker there was any buzzing or rattling, if any. An online audio sweep generator (*Online Tone Generator - Generate Pure Tones of Any Frequency*, n.d.) was used to play audio at frequencies from 10Hz to 300Hz. In addition, various songs and videos with heavy bass were played on the speakers, which allowed us to observe how the speakers might sound when in real-world scenarios.

Sweep Test

Each speaker was audio swept using a MATLAB program provided by our advisor. The MATLAB program creates a signal generator to conduct the sweep and plot the results. The following signal generator graphic pops up when the MATLAB command, guide("Signal_generator_ME2300_rev04.fig"), is entered into the command window.

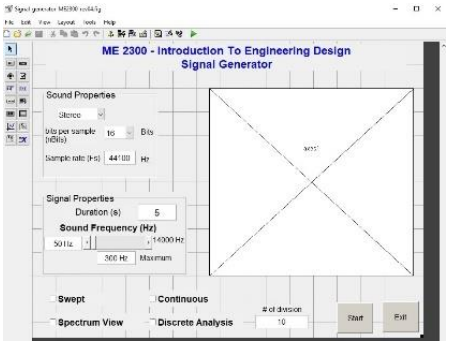

Figure 30: MATLAB sweep popup

When the program is run, the actual signal generator appears. When conducting the sweep tests with both speakers, the duration was set to 10 seconds, the minimum frequency was set to 20Hz, the maximum frequency was set to 300Hz, and the "Swept" and "Spectrum View" options were selected. For each speaker, sweep tests were done with the microphone directly in front of one of the active cones, one of the passive radiators, and about 1.5 feet away from the whole speaker. Doing this gave us readings that focused on the active cones and passive radiators separately as well as gave us readings of the speakers as a whole.

5 Results

5.1 Strain Gauge

5.1.1 Iteration 1

The first round of strain gauge tests was done with the old setup that was controlled with a rheostat. The actuator was swept through the range of approximately zero to twenty volts at various lever arm angles. The max force measured was about 550 grams.

5.1.2 Iteration 2

The second round of strain gauge tests were done with a DC power supply and voltage and current data was collected. A spring constant test was also done which consisted of the actuator force being measured at various angles without powering the actuator. During the powered test, the relationship between force and voltage was measured at deflections between 0 and 10 mm. It was found that the force applied was not dependent on the deflection of the arm. It was also noted that both prototypes showed similar force vs voltage curves, indicating that our production method was consistent and reliable.

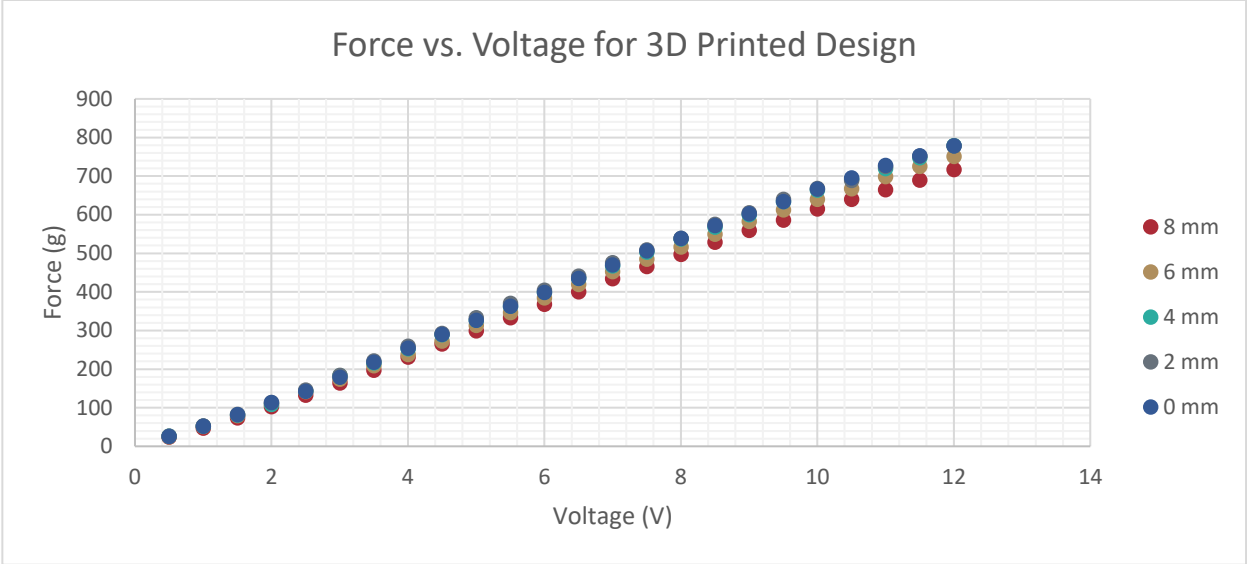

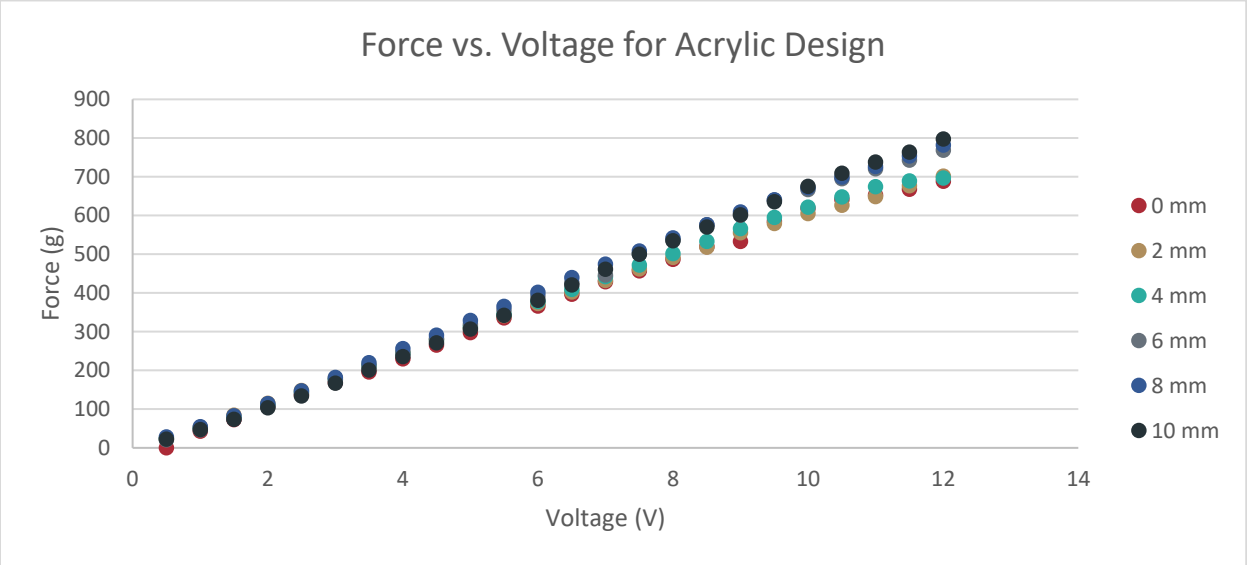

Figure 31: Force vs voltage graphs for both actuators.

The force of the actuator at various levels of deflection was measured without any current passing through the stators. This test gave us a spring constant of about 723 N/m.

5.2 FEA

A static structural analysis of the actuators lever arm was done using Ansys. The arm with magnets was imported into Ansys from Fusion. The arm was assigned to PLA and the magnets to Steel. The arm was constrained using a force at each end of the arm where the speaker cones would be in contact as well as counteracting forces at the top face of the magnets. The center of the arm was constrained as a bearing joint allowing rotation. The total deformation and equivalent stress results can be seen below.

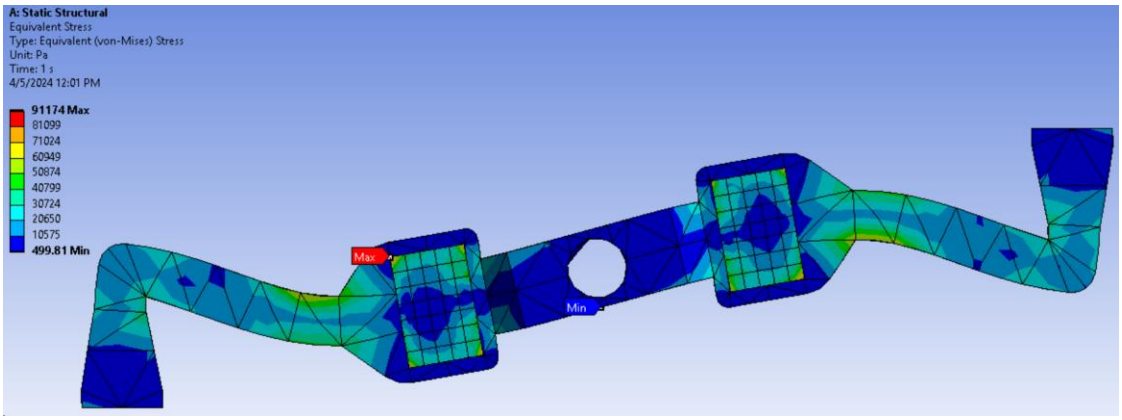

Figure 32: Equivalent stress of lever arm

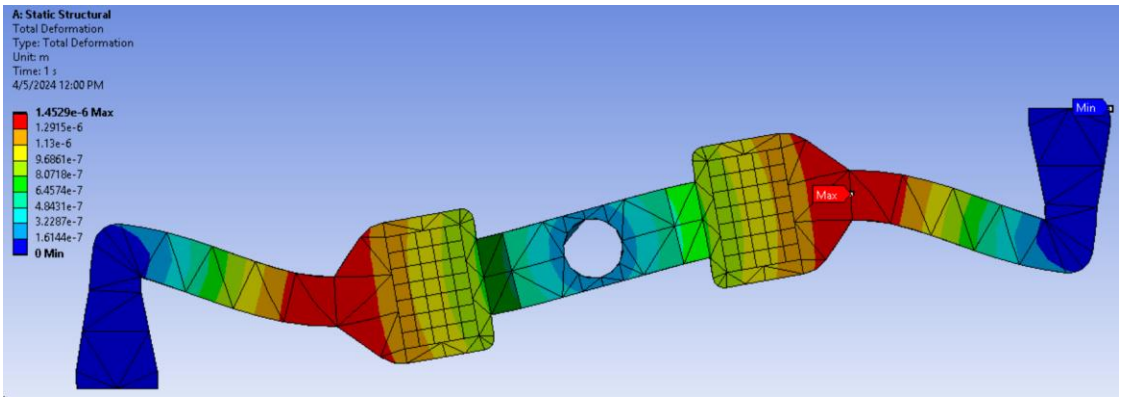

Figure 33: Total deformation of lever arm

5.3 SLDV

The frequency responses of both the 3D printed speaker and the acrylic speaker were recorded and plotted in Excel. The SLDV measures the velocity of the speaker, but it can extrapolate the acceleration, which is more indicative of the audio frequency response of the speaker.

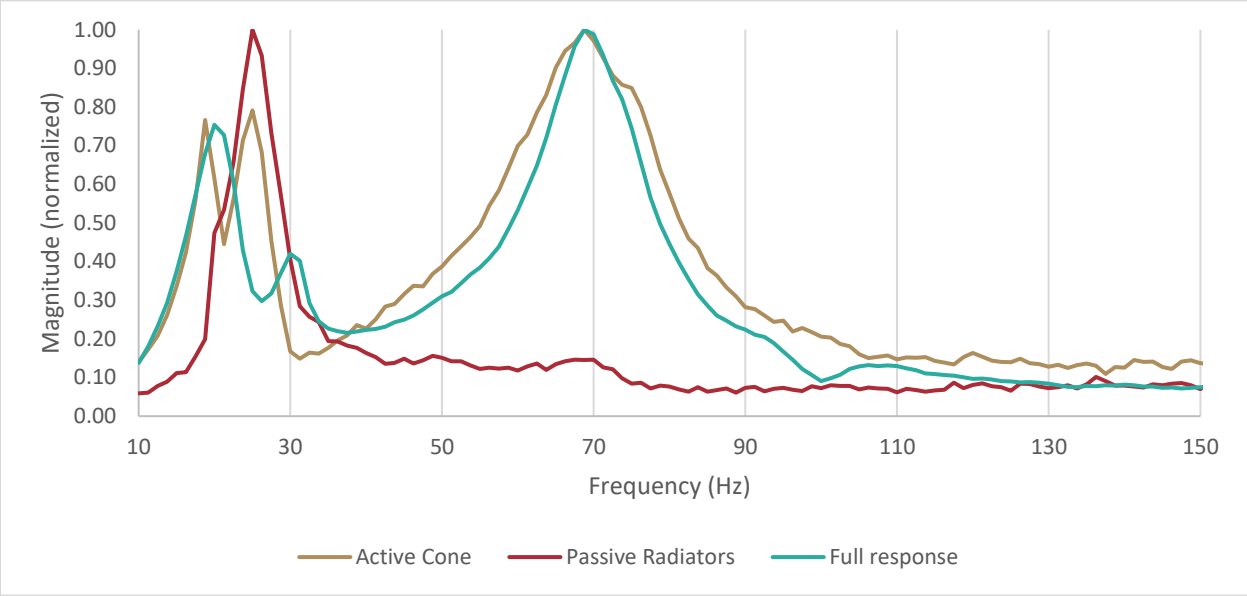

Figure 34: Frequency response of active cone, passive radiator, and full system of the acrylic box with two weights on each passive radiator.

With the acrylic speaker and the 3D printed speaker, we collected a full frequency response of the entire system as well as the response with just the active cone and the passive radiators. Using these, we were able to characterize how the weights affected the resonance of the speaker. As seen in Figure 34, the peak at the lower frequency is caused by the resonance of the passive radiators while the peak at the higher frequency is caused by the active cone.

It was noted that at the lower frequency resonance, the active cone and passive radiators were out of phase, while, at the higher frequency resonance, they were in phase (Figure 35). Out of phase resonance is

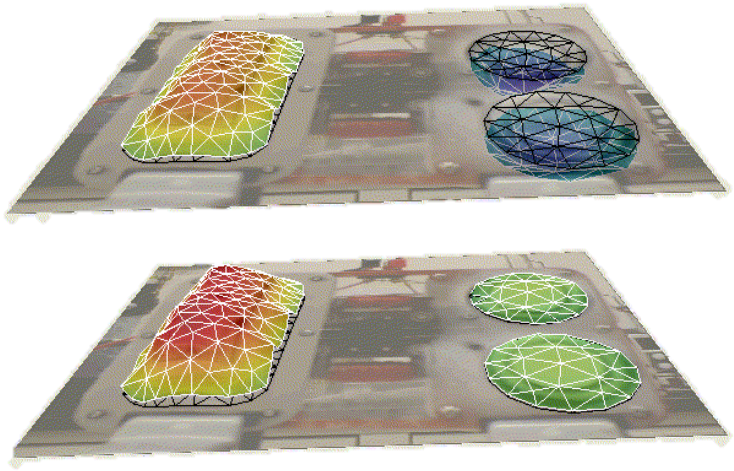

Figure 35: Acrylic speaker box with two weights out of phase resonance at 20.0Hz (top) and in phase resonance at 68.8Hz (bottom).

undesirable because it leads to canceling sound waves coming from the active cone and passive radiators. Because of this, during tuning, we aimed to lower the resonance of the higher frequency peak.

5.3.1 Effect of passive radiator weight

It was found that the passive radiator weight has a significant effect, up to a certain point. As seen in Figure 36, as weight was added to the passive radiators, the higher frequency resonance lowers in frequency and increases in magnitude. With no extra weight on the passive radiators, the active cone resonated at 78.75Hz. This lowers to 73.75Hz with one weight, and it lowers even further to 68.75Hz with two weights. With three weights, though, the peak resonance of the active cone stays at 68.75Hz.

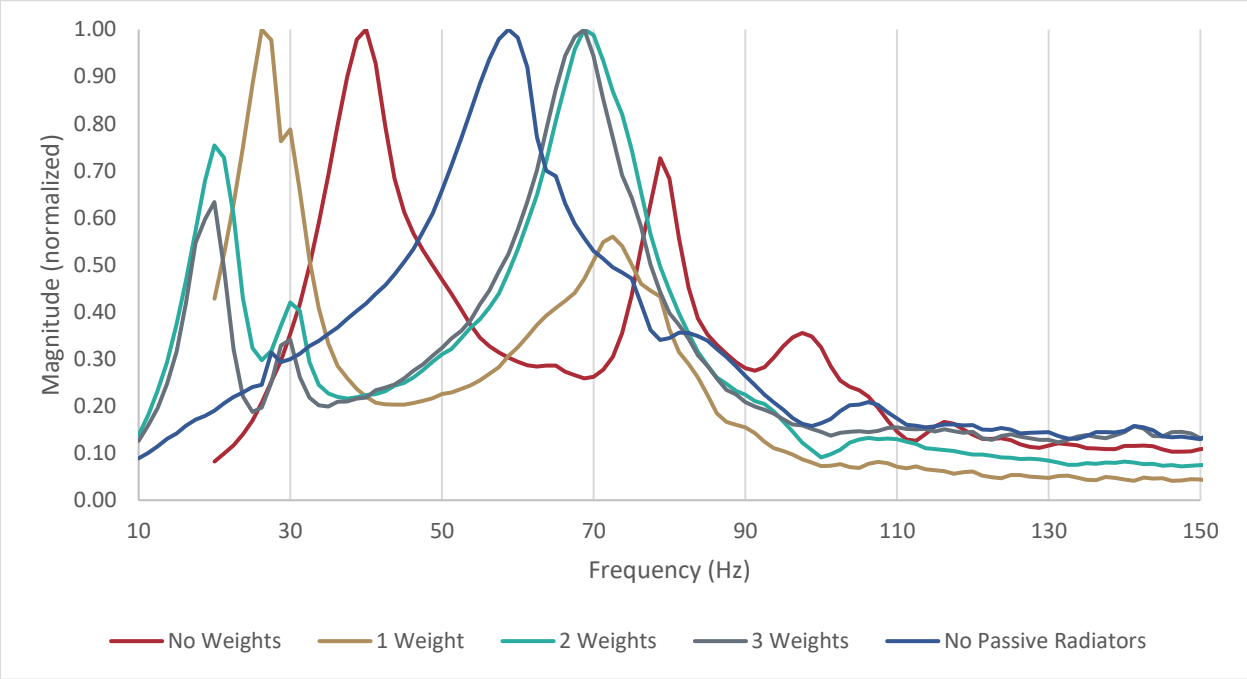

Figure 36: Frequency response comparison between passive radiator weight

When the passive radiators were removed and replaced with a flat plate, the resonance is found at 58.75Hz. As the immovable plate can be assumed to be a passive radiator of infinite mass, it makes sense that the resonance lowers.

5.3.2 Comparison between speakers

As the frequency responses of multiple speakers were collected, we compared the audio qualities of our prototypes to a commercially available bass box. The commercially available box was significantly larger than the two LPHS prototypes. It consisted of two active cones and four passive radiators. As seen in Figure 28, the active cone for the commercial speaker has a wide range of resonance compared to the distinct peaks seen with our prototypes. This is heard audibly as the commercial speaker has a constant volume as it is swept through frequencies, while our prototypes increase in volume significantly at these peaks. While this is undesirable, the low resonant frequency that these prototypes achieved is still admirable for their size.

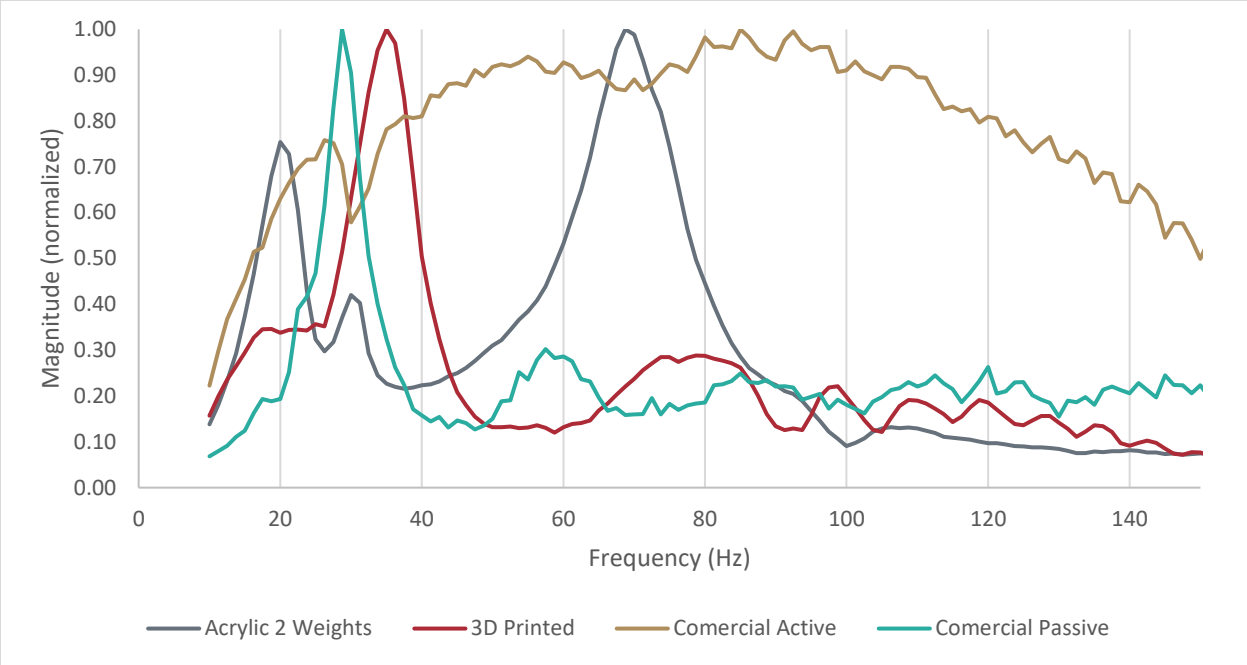

Figure 37: Frequency response comparison between commercial speaker, 3D printed prototype, and acrylic prototype.

The passive radiators of the 3D printed speaker resonated at 35Hz, and the active cone resonated at 73.8Hz. This is only slightly lower than the 40Hz and 78.5Hz found with the acrylic speaker without extra weights on the passive radiators. The lower resonance is likely due to the 3D printed speaker having a slightly larger internal volume.

5.4 Audio and Sweep

We conducted a series of sweep tests to read the frequencies of the active cones and passive radiators of our 3D printed speaker and our acrylic speaker. Some of these tests included putting weights on the passive radiators and/or conducting the test from a distance. The results of these sweep tests are included in Appendix 3. We observed peaks at specific frequency values which correspond to the resonant frequencies of the speaker. The higher the peak, the more audible the sound produced by the speaker is.

After comparing the results of these tests, we observed a difference in the resonant frequencies of the 3D printed and acrylic speakers. On average, the 3D printed speaker had lower resonant frequencies in the tests with no weights, whereas the acrylic speaker had lower resonant frequencies in the tests with weights added to the passive radiators. Ideally, our speakers would have fewer peaks and instead have more consistently audible sound. This is something to improve on in future designs.

6 Conclusion

During this project, two speaker box designs were developed. One was designed to be made from two large 3D prints while the other was designed to incorporate laser cut acrylic plates for much of its structure. Both speakers were proven to be airtight, allowing the use of passive radiators. Along with these

two boxes, two identical moving magnet levered transducers were developed to actuate the speaker cones in the speakers.

The force production and spring constant of the actuators were measured with a strain gauge. Both actuators were determined to have similar force production, indicating that they would perform similarly in the speaker boxes, and that our manufacturing and assembly procedures were consistent.

With the completed speaker boxes and actuators, we assembled two functional prototypes which we tested the audio qualities of. This was done with a custom MATLAB program and an SLDV. Through these tests, we were able to determine the frequency responses of both speakers. With the SLDV, we found that the speakers showed two peaks of resonance. One peak, observed between 20 and 40Hz, was found where the passive radiators resonated while the second peak, observed between 60 and 80Hz, was observed where the active cone resonated. As weight was added to the passive radiators, both peaks lowered in frequency.

While the speakers were shown to resonate in the desired frequency range, the peaks meant that the sound produced by the speakers would increase in volume within these frequency ranges, which is undesirable for use in music or theater systems.

Overall, the main goals of this project were completed. The speaker enclosures were made to be airtight, allowing for the use of passive radiators. The actuator assembly was made significantly stronger, preventing the actuator arm from crashing into the stators. Finally, the effects of passive radiators were studied using the completed prototypes.

7 Discussion

7.1 Broader Impacts/Ethics

Throughout the duration of our project, we made sure to follow the Mechanical Engineering Code of Ethics: an article within the constitution of the American Society of Mechanical Engineers. We made sure to obey each of the fundamental canons and uphold the fundamental principles to the best of our ability.

When manufacturing our speaker, we made sure to follow all the recommended safety protocols. For example, we conducted research on which materials were able to be laser cut before settling on acrylic for one of our speaker boxes and silicone for its gaskets.

Our project could positively impact individuals by allowing subwoofers to be used by those who do not have the space for a traditional commercial subwoofer or do not like the look of having a subwoofer in the open. However, the current design would need adjustments to be feasibly mass produced at a reasonable cost and sold as a consumer product.

7.2 Recommendations for Future Work

With the two prototypes that were developed during this project, we have proven that a moving magnet levered loudspeaker is possible, but there is still a great deal of work to be done to make these designs truly viable before it can be developed as a product. The most important work to be done with the speakers is to continue tuning them to have a good quality of sound and range of resonance. This will likely involve

determining how the rotating actuator fits into acoustic models of speakers with passive radiators. The effect of the volume of the box as well as changes to the weight and shape of the passive radiators should be studied to determine how to best improve the sound quality of the speaker.

Another area to continue work on is improving the power of the actuator. As the torque that the actuator can apply directly influences the volume of the speaker, any improvements that can be made to the power of the actuator will be beneficial. One method for achieving this is reducing the distance between the stators and the permanent magnets on the lever arm. This will likely require an even more robust design to hold the stators, as well as a stronger material than PLA for the lever arm to prevent bending and to better hold the magnets in place.

Finally, the speaker could use some improvements in manufacturability. While we focused on improving the manufacturability of the speakers, we were designing for 3D printing and laser cutting. These methods are not generally viable for the large-scale manufacturing that would be required for a product. One method that could be studied is injection molding. Another way to improve manufacturability is to integrate the base into the speaker box so that the stators and lever arm directly connect to the enclosure rather than requiring a separate base part.

Bibliography

Carlmark, R. T., Chick, G. C., Lucas, B. M., Schroeder, T. C., & Stabile, J. A. (2012). *Moving magnet levered loudspeaker* (United States Patent US8295536B2). https://patents.google.com/patent/US8295536B2/en

McLean, A., Nunes, A., Martin, J., Puksta, J., & Neamtu, A. (2023, April 26). *Low Profile Home Speaker*. Worcester Polytechnic Institute.

Motler, E. J., Kral, J. K., DeLo, J. G., & Rosati, M. A. (2021, May 4). *Low Profile Home Speaker*. Worcester Polytechnic Institute.

Online Tone Generator—Generate pure tones of any frequency. (n.d.). Retrieved April 1, 2024, from https://www.szynalski.com/tone-generator/

Zuber, T., Green, B., Farrah, E., & Rankin, J. (2022, April 27). *Designing a Low-Profile Home Speaker Utilizing a Moving Magnet Transducer*. Worcester Polytechnic Institute.

Appendix 1: Cone Molding Process

Step 1. 3D-print the center plate of the cone and the top and bottom halves of the mold.

Figure 38: Top half of the mold (top) and bottom half of the mold (bottom).

Step 2. Acquire silicone lubricant, parts A & B of liquid silicone, a vacuum chamber (1 bar of pressure minimum), and six M5 nuts and bolts. Make sure the bolts are long enough to go through the whole mold.

Figure 39: Silicone lubricant (top left), six M5 nuts and bolts (top right), vacuum chamber (bottom right), and parts A & B of liquid silicone (bottom left).

Step 3. Apply silicone lubricant to the insides of the two halves of the mold (we used Blaster Silicone Lubricant: https://blasterproducts.com/product/silicone-lubricant). Let the pieces sit for 5 minutes.

Step 4. Open part A and part B of the liquid silicone (we used Dragon Skin 10 Medium: https://www.smooth-on.com/products/dragon-skin-10-medium). Mix equal amounts of part A and part B into a cup. We used about 60 grams of each part. Stir for 1 minute.

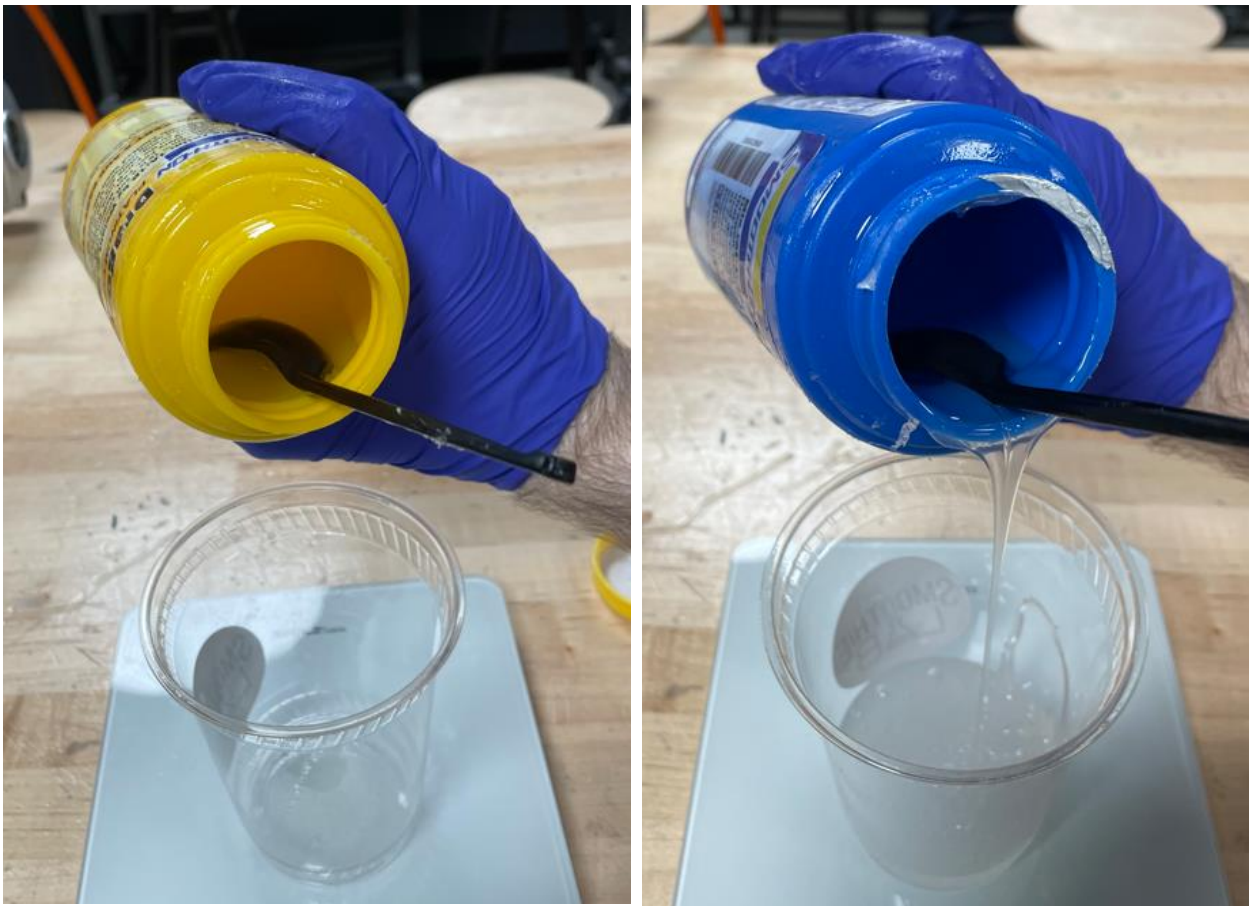

Figure 40: Part A (left) and part B (right) of liquid silicone.

Step 5. Take out the vacuum chamber. Insert the center piece of the cone into the bottom half of the mold. Then, insert the bolts into the bottom half of the mold with the threads facing upwards. Lastly, place the bottom half of the mold, with the center piece and bolts inserted, into the vacuum chamber.

Figure 41: Mold with inserted center piece (top left), mold with inserted center piece and screws (bottom left), mold inside vacuum chamber (right).

Step 6. Pour the silicone mixture into the bottom half of the mold.

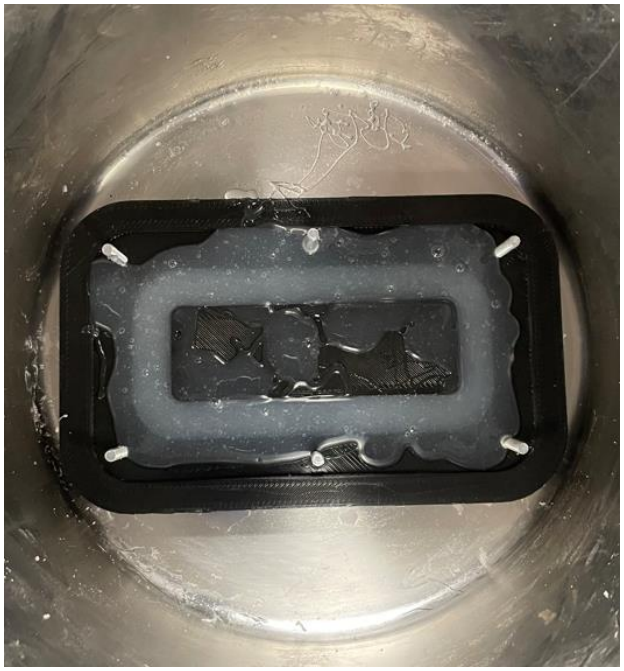

Figure 42: Silicone mixture in mold in vacuum chamber.

Step 7. Turn on the vacuum chamber for about 5-10 minutes.

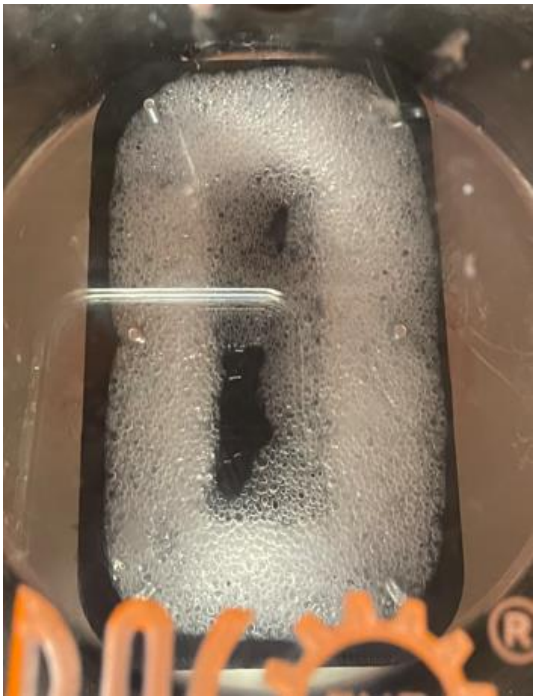

Figure 43: Air being removed from the silicone mixture.

Step 8. Place the top half of the mold onto the bottom half so that the bolts go through their respective holes in the top half.

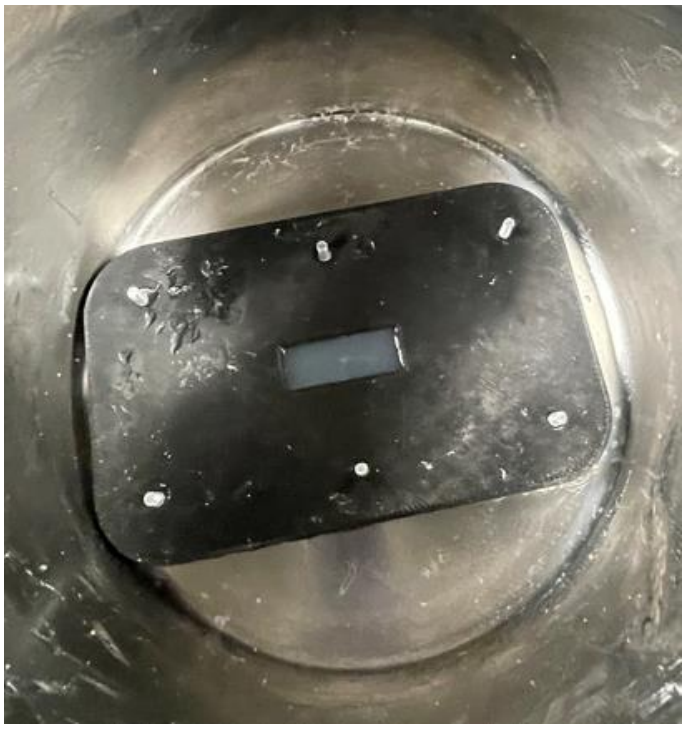

Figure 44: Mold in vacuum chamber with top half added.

Step 9. Carefully remove both halves of the mold from the vacuum chamber, making sure the bolts don't fall out and the silicone doesn't spill.

Figure 45: Mold after being removed from the vacuum chamber.

Step 10. Fasten the two halves of the mold together by screwing the nuts onto the bolts.

Figure 46: Mold with nuts added to screws.

Step 11. Let the mold sit for 24 hours.

Step 12. Unscrew the nuts from the bolts, separate the two halves of the mold, and remove the finished silicone speaker cone. You may need to pry the two halves of the mold apart using a screwdriver or similar wedge.

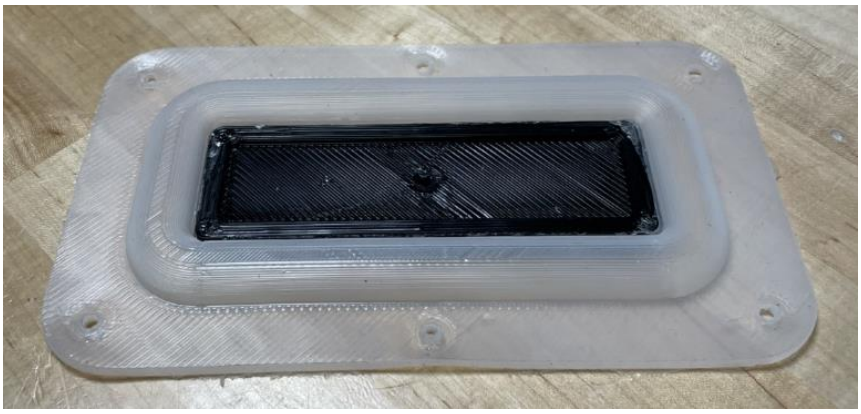

Figure 47: Finished speaker cone.

Appendix 2: Actuator Force Testing

This appendix describes the procedure to test the force of the actuator assembly.

Equipment

- Arduino Uno
- DC Power Supply
- Strain Gauge
- Jumper Cables
- Micrometer

Setup

Use the strain gauge setup provided by Professor Stabile. Clamp the actuator down to the setup so it does not move. Connect the Arduino to the strain gauge and connect the Arduino to a computer. Then, connect one wire of the actuator to the positive terminal in the power supply and the other wire to the negative terminal of the power supply.

Calibration

Before running the experiment, the strain gauge needs to be calibrated to obtain the most accurate results. To do this, connect the Arduino to the computer and start a program to read the value from the strain gauge. Place known masses on the strain gauge and record what the Arduino is reading for each in an excel spreadsheet. Once enough masses are tested, create a scatter plot with the measured mass on the x-axis and the true mass on the y-axis. Add a trendline and show the equation of the trendline. In the Arduino code, multiply the output from the Arduino by the slope of the trendline and add the intercept value. Retest with the known masses to check whether the calibration worked.

Experiment

After finishing the calibration, place the actuator under the strain gauge and move the strain gauge so it is just touching the end of the actuator arm. Turn on the DC power supply after making sure the actuator is disconnected or the output is off. Set the current limit to the maximum value that the DC power supply allows and set the voltage to 0.5V. Start the Arduino program and wait for values to start showing up. Once the Arduino is taking in values, connect the output of the DC. It is recommended to use a DC power supply with a separate output switch or place a switch in the circuit to prevent dangerous electrical arcing. Record the force that is being applied and the current that the power supply is drawing and then disconnect the power supply. Restart the Arduino program and turn the voltage on the DC power supply up to 1V. Repeat the test at 0.5V increments until reaching 12V.

After measuring up to 12V, using the micrometer, push the actuator arm down 2mm. Repeat the experiment from 0.5V to 12V, recording force and current. Continue to repeat the experiment with 4mm, 6mm, and 8mm of vertical displacement.

Appendix 3: Audio Sweep Testing Data

3D Printed

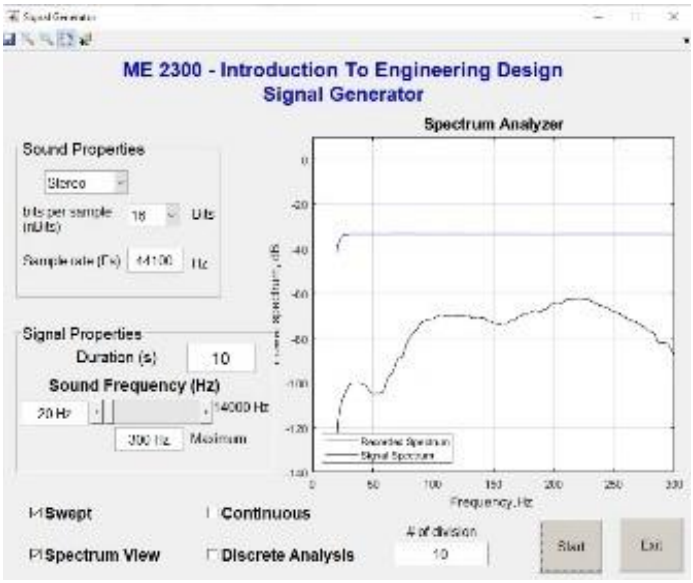

Figure 48: 3D Printed Active Cone Sweep Experiment 1

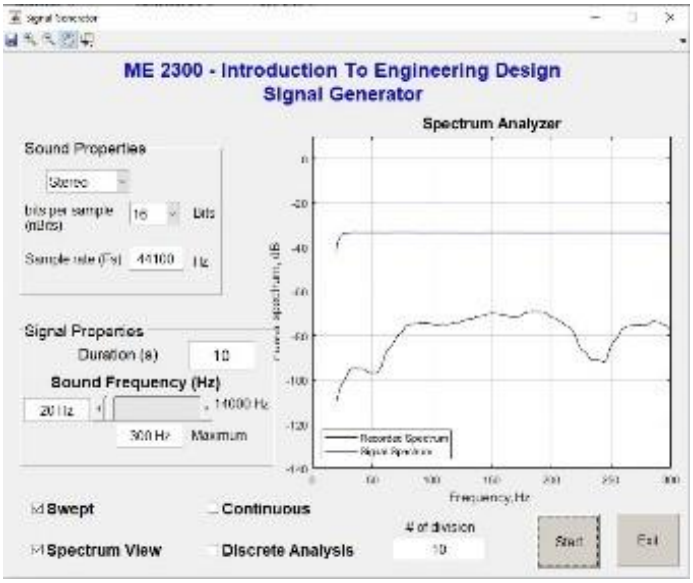

Figure 49: 3D Printed Passive Radiator Sweep Experiment 1

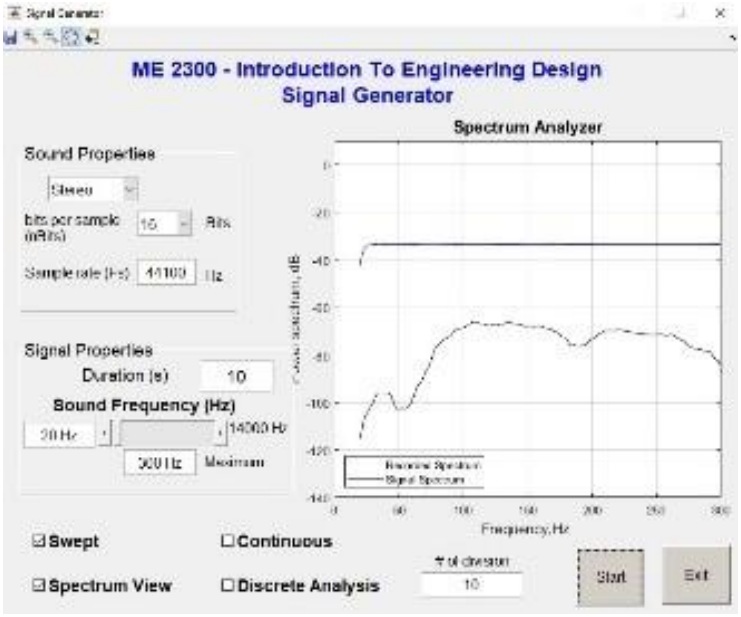

Figure 50: 3D Printed Active Cone Sweep Experiment 2

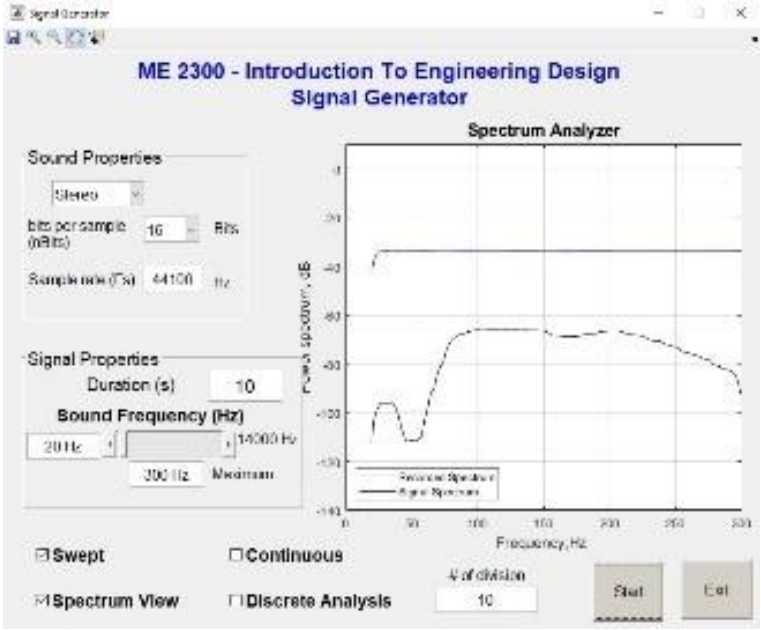

Figure 51: 3D Printed Passive Radiator Sweep Experiment 2

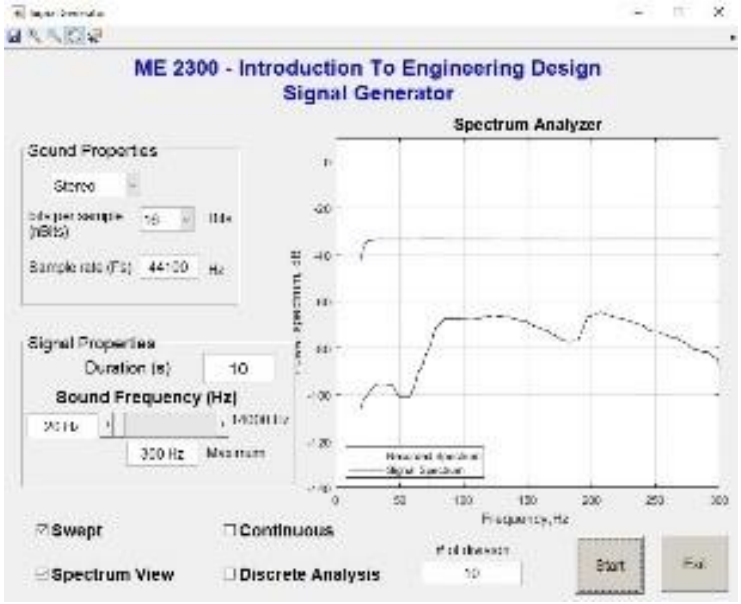

Figure 52: 3D Printed Active Cone Sweep Experiment 3

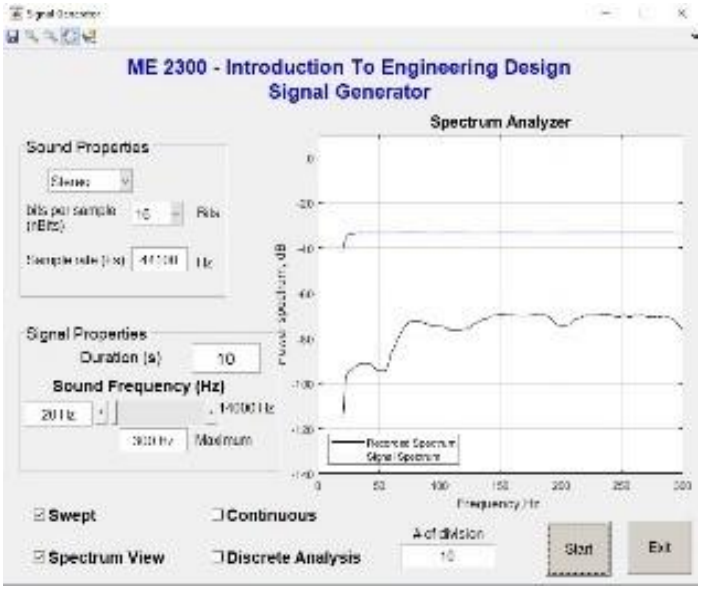

Figure 53: 3D Printed Passive Radiator Sweep Experiment 3

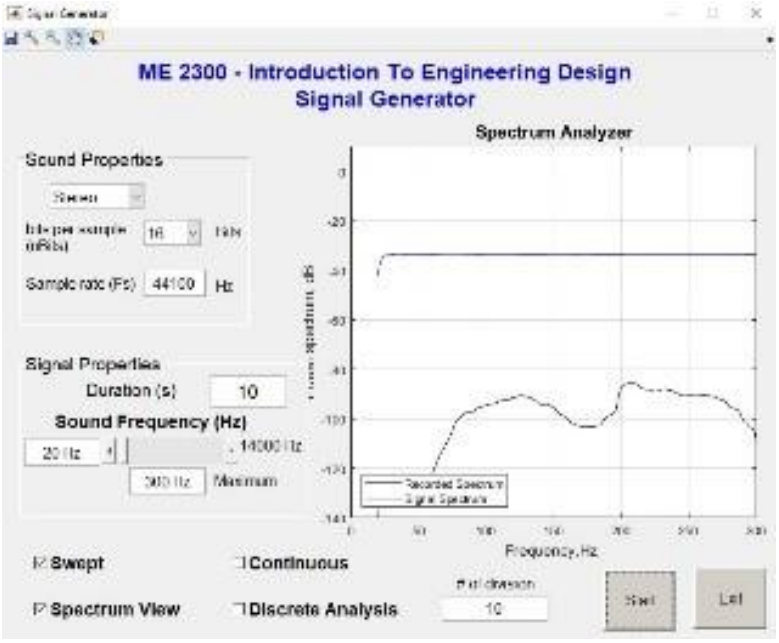

Figure 54: 3D Printed Sweep Test at About 1.5 ft Away

Acrylic

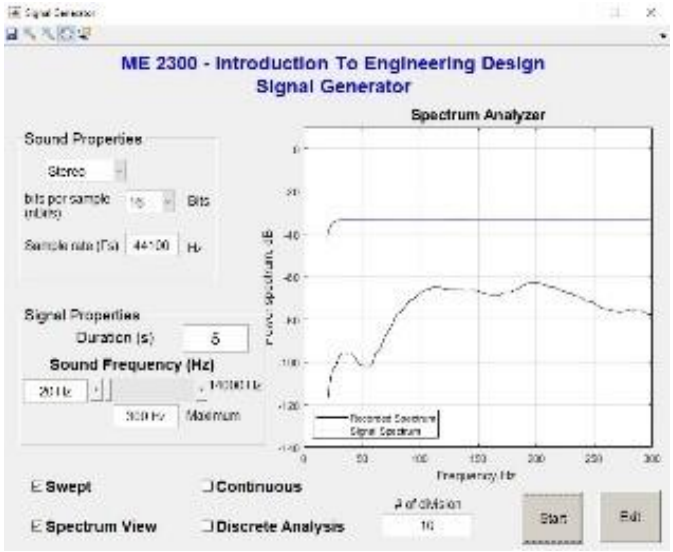

Figure 55: Acrylic Active Cone Sweep With No Weights on Passive Radiators

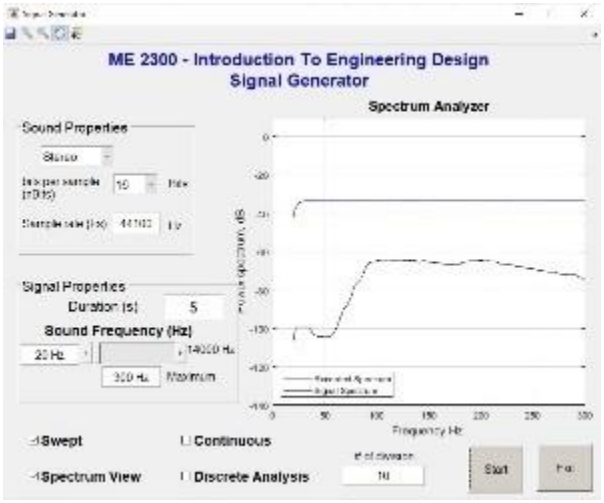

Figure 56: Acrylic Passive Radiator Sweep With No Weights on Passive Radiators

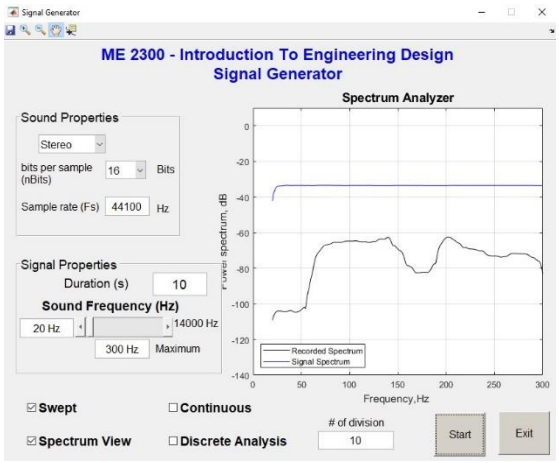

Figure 57: Acrylic Active Cone Sweep With 2 Weights on Passive Radiators Experiment 1

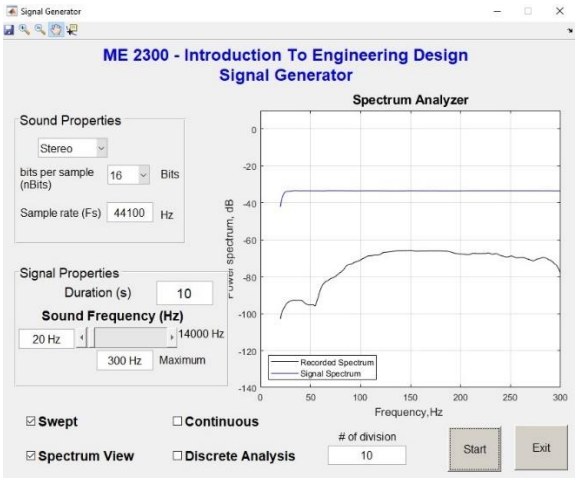

Figure 58: Acrylic Passive Radiator Sweep With 2 Weights on Passive Radiators Experiment 1

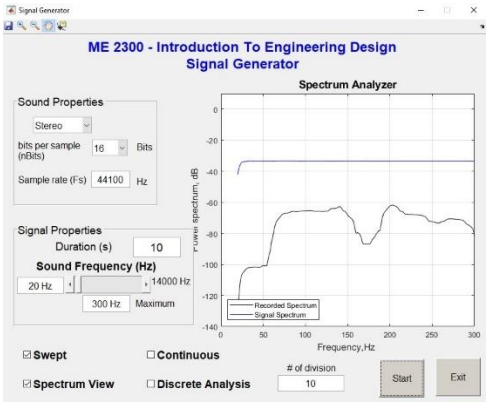

Figure 59: Acrylic Active Cone Sweep With 2 Weights on Passive Radiators Experiment 2

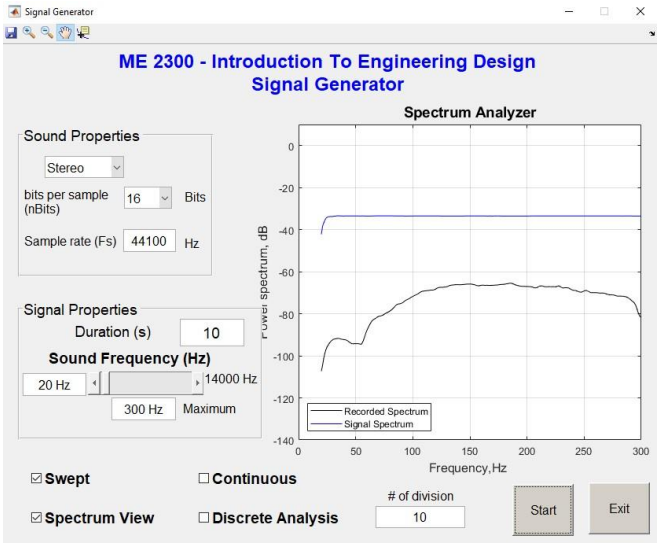

Figure 60: Acrylic Passive Radiator Sweep With 2 Weights on Passive Radiators Experiment 2

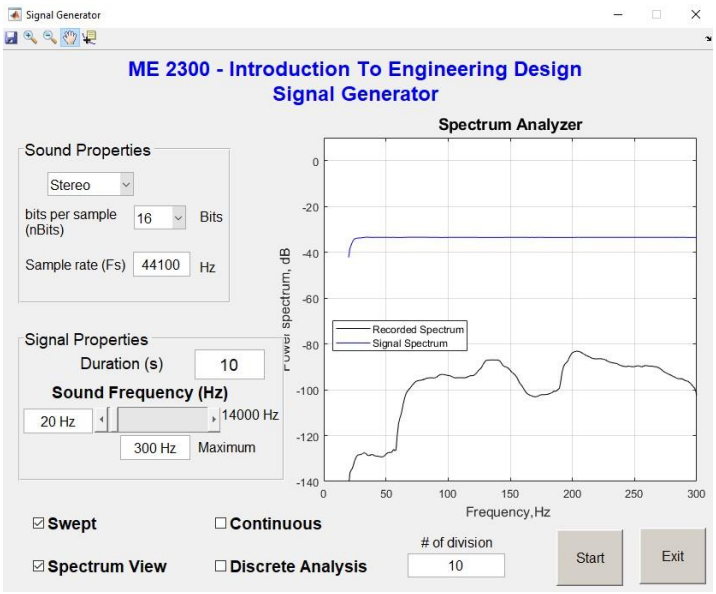

Figure 61: Acrylic Sweep Test at About 1.5 ft Away With 2 Weights on Passive Radiators

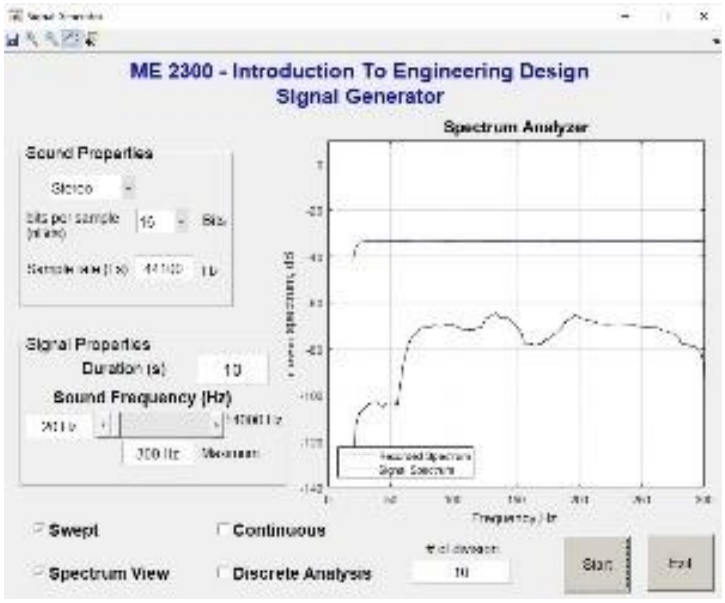

Figure 62: Acrylic Active Cone Sweep With 3 Weights on Passive Radiators Experiment 1

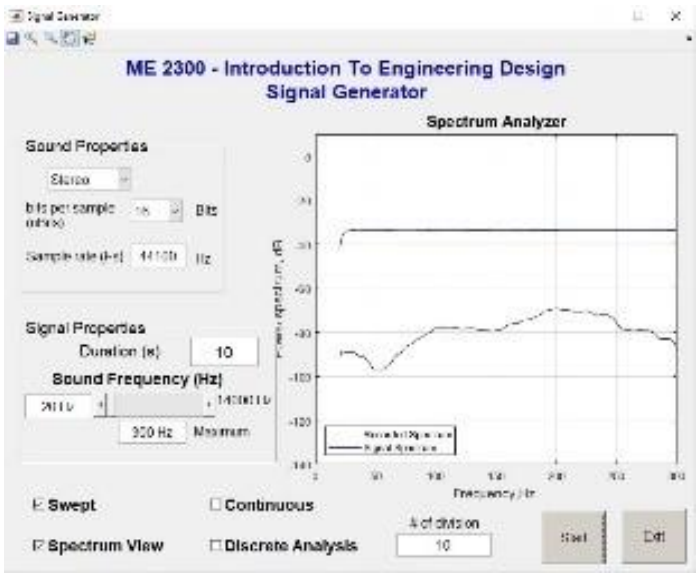

Figure 63: Acrylic Passive Radiator Sweep With 3 Weights on Passive Radiators Experiment 1

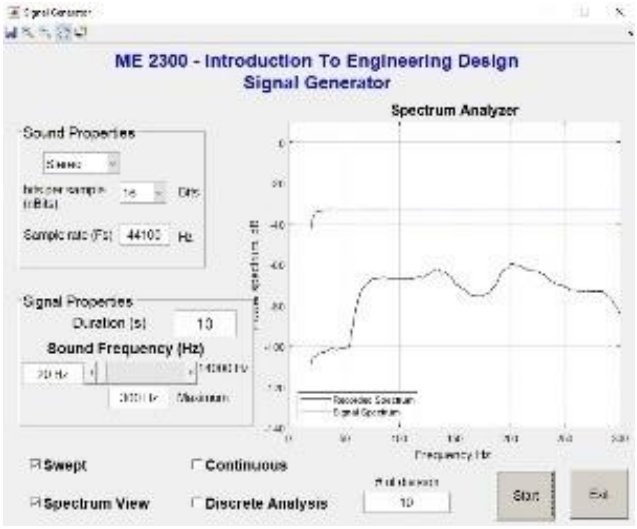

Figure 64: Acrylic Active Cone Sweep With 3 Weights on Passive Radiators Experiment 2

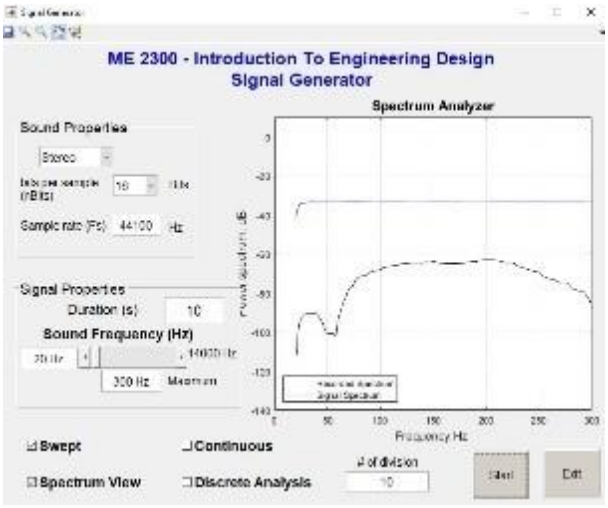

Figure 65: Acrylic Passive Radiator Sweep With 3 Weights on Passive Radiators Experiment 2

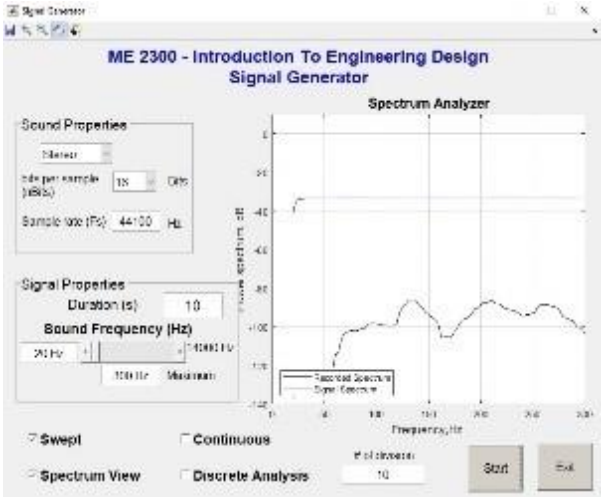

Figure 66: Acrylic Sweep Test at About 1.5 ft Away With 3 Weights on Passive Radiators